Politecnico di Torino

Master's degree in Georesources and Geoenergy Engineering

A.Y. 2025/2026

Groundwater flow and heat transport modelling of a district-scale shallow geothermal system in Milan

Advisors:

Prof. Alessandro Casasso

Ms. Maria Adele Taramasso

Candidate:

Shehabeldeen Baher

ID: 301192

Acknowledgments

First and foremost, I thank God for His guidance to complete this thesis.

I am deeply grateful to Professor Alessandro Casasso for his mentorship and guidance throughout the field that I chose to explore in depth, renewable geothermal energy. His approachable, collaborative, and understanding nature made this journey both productive and bearable.

My sincere thanks go to all my professors and staff at Politecnico di Torino for their inspiring teachings, and special thanks to Ms. Maria Adele Taramasso who gave me a hand at many stages of this work.

I am also truly grateful to Italy, a welcoming and inspiring country, that made my academic experience both enriching and memorable.

Finally, my heartfelt love goes to my friends for their constant support and encouragement, and simply for being there whenever I needed a break; you are the true treasure of the journey.

Table of Contents

Abstract

With a lower carbon footprint than traditional heating and cooling systems, shallow geothermal systems are becoming increasingly popular. However, to prevent overexploitation and detrimental effects on already-existing structures and installations, shallow subsurface exploitation needs to be carefully considered.

This thesis examines the thermal impact of installing a groundwater heat pump system in a district in Milan with an overall thermal power 56 MW and an annual production of about 134 GWh/year.

Available geological and hydrogeological data were examined to construct a coupled groundwater flow and heat transport numerical model using the finite-element software FEFLOW. Using monthly time steps, the plant's operation was simulated with thermal loads estimated from the characteristics of the buildings.

The results show that, with the full injection of groundwater after the heat exchange, the thermal impact is not sustainable as groundwater temperatures would fall below 0°C.

However, removing four injection wells (approximately 36% of the overall reinjection flow rate), and replacing them with surface discharge through surface channels, would mitigate the thermal impact, making it possible to meet the entire thermal demand of the district using a groundwater heat pump system.

1 Introduction

As global demands for sustainable and low-carbon energy sources increase, geothermal energy has become a promising and renewable option for heating, cooling, and power generation. In contrast to other renewable energy sources, geothermal energy provides a consistent and reliable energy supply, it is not dependent on climate conditions as wind or solar energy. As a result, base load can be provided which helps to lessen reliance on fluctuating energy markets and reduce greenhouse gas emissions.

Geothermal energy utilizes the heat stored beneath the Earth's surface for a variety of purposes, such as generating electricity and providing direct heating. This energy is derived from the Earth's core as well as the natural radioactive decay of minerals found in the crust.

This thesis deals with an open loop system for heating and cooling of a district scale shallow geothermal system in Milan. The first section presents information on shallow geothermal systems, open and closed loop systems, heat pumps, thermal and hydraulic recycling and related parameters. Section 2 analyses the case study from regional (Milan) to district scale, hydrogeological point of view and aquifer parameters, monitoring groundwater level in Milan, evolution of groundwater levels and interactions with underground structures. Section 3 focuses on the simulation of the plant operation through subsurface flow and heat transport modelling with FEFLOW, examines the existence of thermal impact of installing a groundwater heat pump. Section 4 summarizes the results of the work and the conclusions that can be drawn from them.

1.1 Geothermal Energy

1.1.1 Definition

Geothermal energy refers to the heat that originates from the Earth, specifically from the thermal energy found in the rocks and fluids that occupy the fractures and pores within the Earth's crust.

Geothermal resources are classified based on:

- Heat Source:
    - low-temperature (T < 90 °C) or low-enthalpy resources.

- middle-temperature (T ≈ 90–150 °C) or medium-enthalpy resources.
- high-temperature (T > 150 °C) or high-enthalpy resources.

- Heat Extraction:
  - Deep Geothermal Systems: These high-temperature reservoirs (T > 150 °C) generate steam that drives turbines for electricity production.
  - Shallow Geothermal Systems: These systems make use of stable ground temperatures (T < 90 °C) for heating and cooling through geothermal heat pumps (GHP).

The present study focuses on shallow geothermal systems operating under low-enthalpy conditions.

1.1.2 Geothermal energy: potential and applications

The potential of geothermal energy in Europe is considerable. At present, deep geothermal technology is only deployable in certain areas characterised by high temperatures (geothermal anomalies), but GHP can be used virtually everywhere the rapid growth in geothermal energy deployment over time clearly demonstrates its increasing importance (Fig. 1).

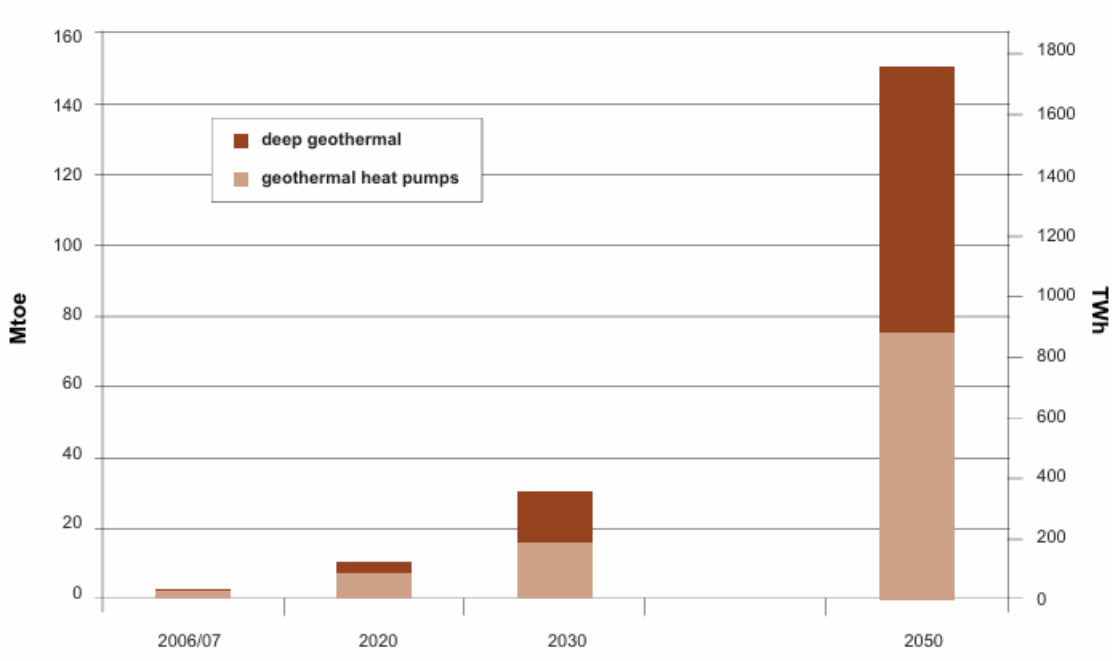

Figure 1 - Heating potential of geothermal energy in EU (from [1]).

Geothermal energy is a means of reducing emissions associated with heating and electricity generation compared to fossil fuel-based technologies. Although it is not extensively utilized, it holds significant promise. As reported by the IEA, geothermal energy currently accounts for less than 1% of the global energy demand. Data from Eurostat indicates that geothermal electricity production represents less than 0.25% of the total electricity generated in EU-27 and less than 0.1% of the overall installed electrical capacity. Fig. 2 illustrates geothermal electricity production and installed capacity across the European Union.

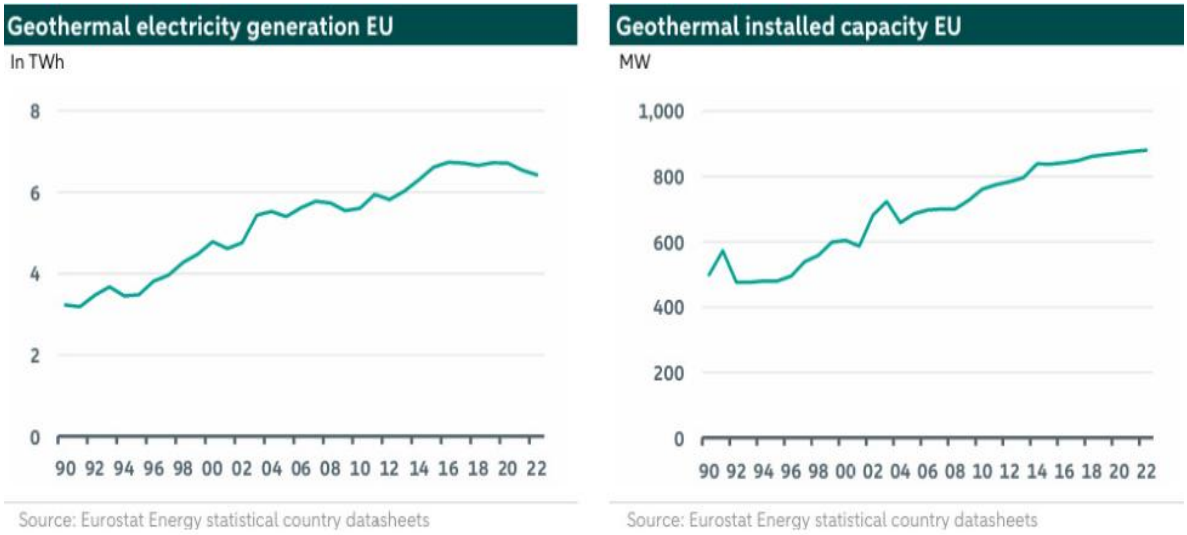

Figure 2 - Geothermal electricity production and installed capacity across the entire EU (from [2]).

By 2050, the combined potential of RES exceeds the heating demand and the long-term scenario with 100% renewable heat energy reduces the emissions of GHG related to consumption of fossil fuels.

Fig. 3 breaks down aggregate RES heat supply into its components and clarify the share of geothermal sources.

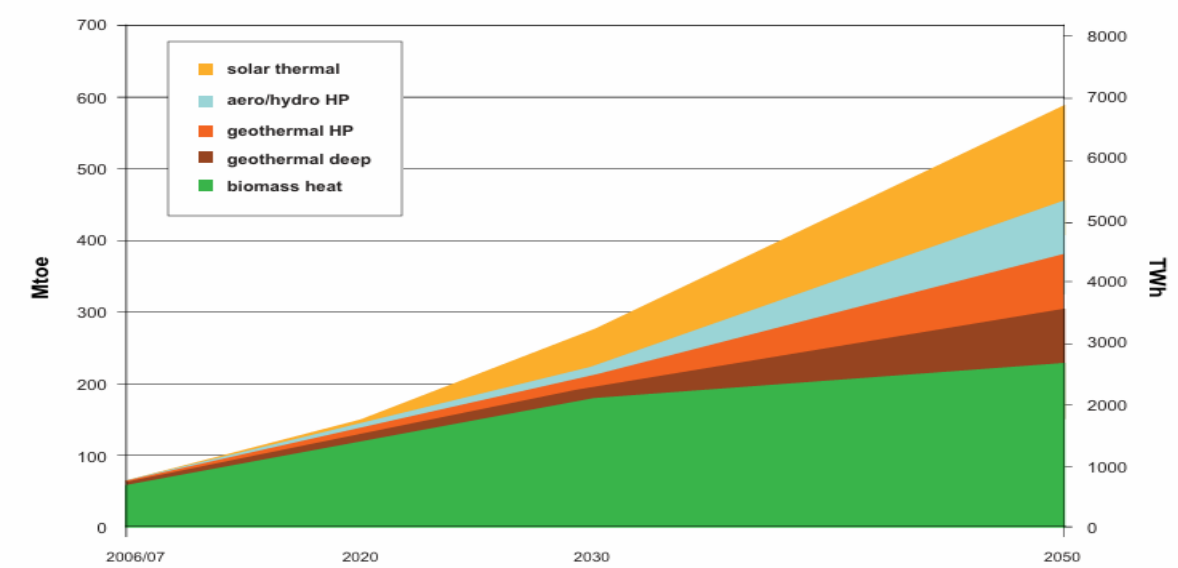

Figure 3 - Heating potential by renewable energy source in EU (from [2]).

1.1.3 Advantages of geothermal energy

Geothermal energy stands out from solar and wind power, which face challenges related to their intermittent nature. It can deliver continuous electricity, heat generation, and storage around the clock, making it a unique renewable energy source. The International Energy Agency (IEA) states that geothermal power can consistently operate at its full capacity throughout both day and night and year-round. In 2023, the capacity factor (i.e., how much energy is produced by a plant compared to its maximum output) of geothermal energy averaged over 75%, in stark contrast to less than 30% for wind and under 15% for solar photovoltaic (PV) systems.

Geothermal energy can also be exploited through heat pump systems, providing several environmental and energy-related advantages. Heat pumps operate without direct pollutant emissions at the point of use and eliminate the need for on-site fuel storage. Furthermore, their operation contributes to a reduction in primary energy consumption and greenhouse gas (GHG) emissions. When heat pumps replace conventional gas-fired boilers for space heating, a significant decrease in emissions can be achieved, with studies indicating a reduction in GHG emissions ranging from approximately 48% to 73%. In addition, the substitution of gas boilers with heat pump systems leads to a reduction in nitrogen oxides (NOx), which are typically associated with combustion-based heating technologies.

1.1.4 Challenges of geothermal energy

Geothermal energy has high upfront costs and considerable operational expenses. Table 1 presents the global weighted average total installed costs in USD per kW. For geothermal energy, these costs are among the highest; only concentrated solar power shows higher values. However, geothermal energy has the highest capacity factor, which represents the amount of energy produced by a plant relative to its maximum possible output. In other words, it indicates how often the plant operates at or near its maximum power. The table also shows that geothermal energy has one of the highest levelized costs of electricity (LCOE).

Global weighted average total installed costs, capacity factor and LCOE

	Total installed costs (2023 USD/kW)			Capacity factor (%)			Levelised cost of electricity (2023 USD/kWh)		
	2010	2023	Percent change	2010	2023	Percent change	2010	2023	Percent change
Bioenergy	3 010	2 730	-9%	72	72	0%	0.084	0.072	-14%
Geothermal	3 011	4 589	52%	87	82	-6%	0.054	0.071	31%
Hydropower	1 459	2 806	92%	44	53	20%	0.043	0.057	33%
Solar PV	5 310	758	-86%	14	16	14%	0.46	0.044	-90%
CSP	10 453	6 589	-37%	30	55	83%	0.393	0.117	-70%
Onshore wind	2 272	1 160	-49%	27	36	33%	0.111	0.033	-70%
Offshore	5 409	2 800	-48%	38	41	8%	0.203	0.075	-63%

Source: IRENA (2024), Renewable Power Generation Costs in 2023, International Renewable Energy Agency, Abu Dhabi.

Table 1- Renewable Power Generation Costs.

For medium and high enthalpy geothermal energy, possible environmental issues are:

- Drilling: noise, blow outs of fluids from wells.
- Tests and operation: release of gas.
- Impact on the ground, in particular subsidence.

1.2 Low enthalpy geothermal systems

Geothermal energy, defined as the utilization of the Earth's internal heat, represents an important renewable energy source (RES). Based on the temperature of the natural fluids involved, resources are generally classified into three categories: high-enthalpy (T > 150 °C), medium-enthalpy (T = 90–150 °C), and low-enthalpy (T < 90 °C). High and medium-enthalpy resources are primarily used for generating electricity as well as for various

direct applications of the used fluids. These resources are typically found in geologically active regions, often associated with volcanic activity, high heat flow, and tectonic plate boundaries or hotspots.

Low-enthalpy resources are mainly utilized for direct applications, which can be accessed in many locations such as geothermal heat pumps, recreational bathing and swimming, space heating, district heating, heating for greenhouses, aquaculture, and applications in agriculture and industry.

A low-enthalpy geothermal energy system (Fig.4) consists of:

- Heat Source (Geothermal Reservoir): Typically located at shallow depths (100–500m) with groundwater or rock formations at moderate temperatures (10–90 °C).
- Heat Exchange System:
    - Open loop: Extracts groundwater directly from wells and returns it after heat exchange.
    - Closed loop: Uses underground pipes filled with a heat-transfer fluid (e.g., water, antifreeze).
    - Heat Pump (for GHP systems): Transfers heat between the ground and buildings. Operates using a compressor, heat exchanger, and refrigerant cycle.

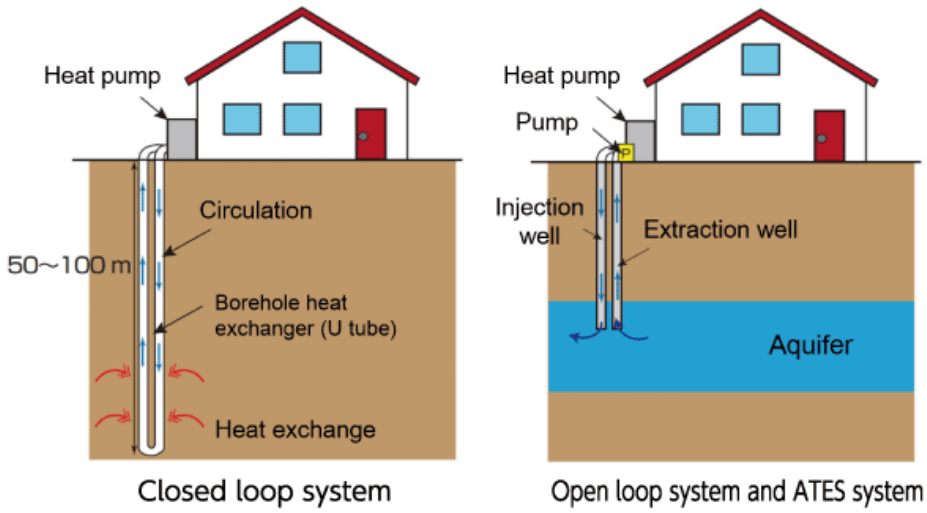

Figure 4 - Low enthalpy geothermal energy systems.

1.3 Heat pumps

The heat pump extracts heat from a source, such as the surrounding air, geothermal energy stored in the ground, or nearby sources of water or waste heat from a factory. It then amplifies and transfers heat from a low temperature source to a high-temperature sink. This process requires external mechanical or thermal energy, through two principles:

- Vapour compression: The increase of pressure (and thus, temperature) is provided by a mechanical compressor, which consumes electrical energy (Fig. 6).
- Absorption: The mechanical compressor is replaced by a thermal source and a binary mix of fluids (aqueous solutions of LiBr or NH_3), in which the most volatile acts as a refrigerant, while the least volatile is a solvent.

The vapour compression heat pump cycle is ideally based on the reversed Carnot cycle; in practice it is more accurately represented on a pressure–enthalpy (P–h) diagram (Fig. 5-a), which illustrates the thermodynamic processes:

- Isothermal evaporation (1-2): The heating fluid absorbs heat and transitions from a saturated liquid state to a saturated vapor state.
- Isentropic compression (2-3): The pressure rises while the saturated vapor becomes superheated.
- Isothermal condensation (3-4): The fluid releases heat and turns back into a saturated liquid.
- Isentropic expansion (4-1): Both pressure and temperature drop, and the fluid returns to its original state.

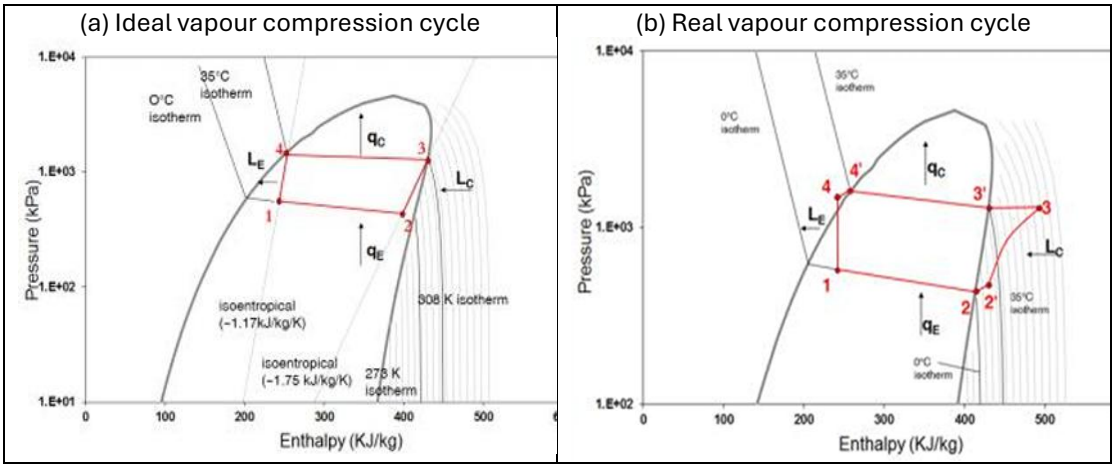

Figure 5 - Pressure–enthalpy (P–h) diagrams of a heat pump: (a) ideal cycle and (b) real cycle showing deviations (from [6]).

However, HP works with a modified reversed Carnot Cycle due to variation in entropy due to expansion and compression (Fig. 5-b), entropy (kJ/kg/°C) is a state variable which describes the level of disorder of matter, it increases in transition from L to V and decreases from V to L.

Additional real cycle processes include:

- Superheating (2-2'): Further heating occurs to vapour comes from evaporator to be sure that vapour is fully saturated.
- De-superheating (3-3'): At the beginning of condensation, the superheated vapour is cooled to the saturation temperature.
- Under cooling of saturated liquid (4-4'): The liquid refrigerant is cooled below saturation to avoid vapour formation before the expansion valve, thereby enhancing system efficiency.

A heat pump consists primarily of a compressor that circulates a refrigerant through a closed refrigeration cycle, along with heat exchangers that facilitate heat transfer between the source and the sink. Heat is extracted from a low-temperature source and delivered to a heat sink through these heat exchangers (Fig. 6).

In buildings, the heat is delivered using either forced air or hydronic systems such as radiators or underfloor heating. HP can be connected to a tank to produce sanitary hot water or provide flexibility in hydronic systems. Many of the heat pumps can also provide space cooling in summer in addition to meeting space heating needs in winter. The heat

carrier fluid which flows in this circuit is called refrigerant, HP exploit the ability of it to absorb and release heat during transition from liquid to vapour and vice versa.

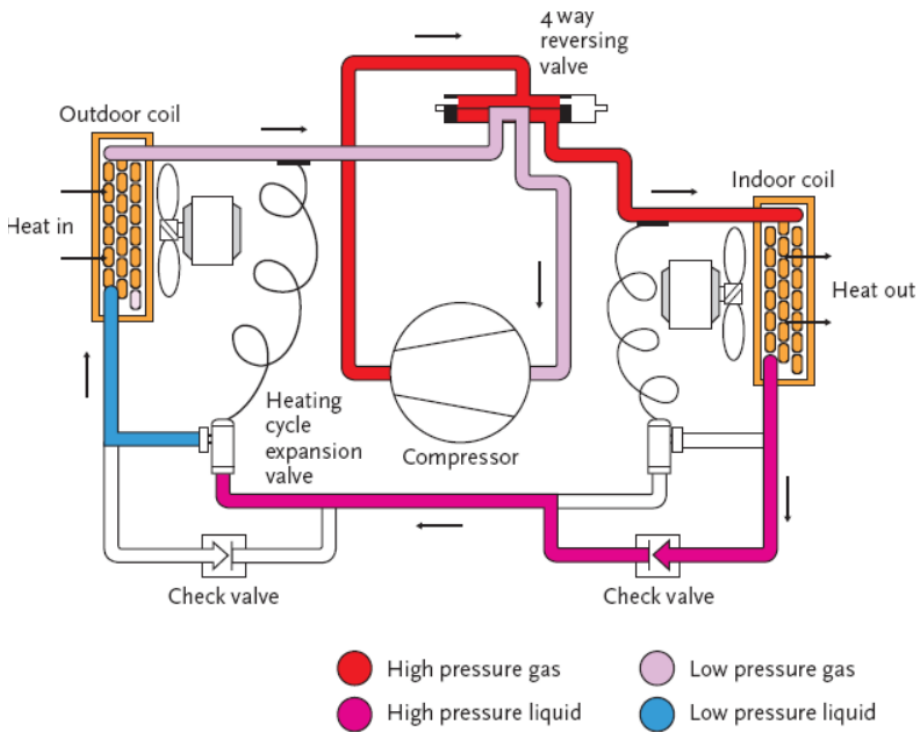

Figure 6 - Reverse cycle heat pump - heating mode (from [7]).

The energy efficiency of the heat pump is called coefficient of performance (COP) and it is defined as the ratio between the useful effect of the heat pump (cooling or heating capacity) and the work spent by the compressor.

COP is used when the useful effect is heating, while the EER (Energy Efficiency Ratio) is used in the case of cooling.

For a reversible heat pump operating between T_1(low temperature heat source) and T_2(high temperature heat sink), expressed in Kelvin and with $T_2 > T_1$, the maximum theoretical COP is:

$$\mathrm{COP}_{\mathrm{heating}} = \frac{T_2}{T_2 - T_1}$$

$$COP_{cooling} = \frac{T_1}{T_2 - T_1}$$

In practical applications, the COP is always lower than the ideal Carnot limit due to system irreversibilities, typical values are:

- Air-source heat pumps: COP ≈ 2.5–3.5
- Ground-coupled heat pumps: COP ≈ 3.5–4.5
- Groundwater heat pumps: COP ≈ 4–5

These ranges are consistent with values reported in the literature (Lund et al., 2011; IEA, 2022; ASHRAE, 2020).

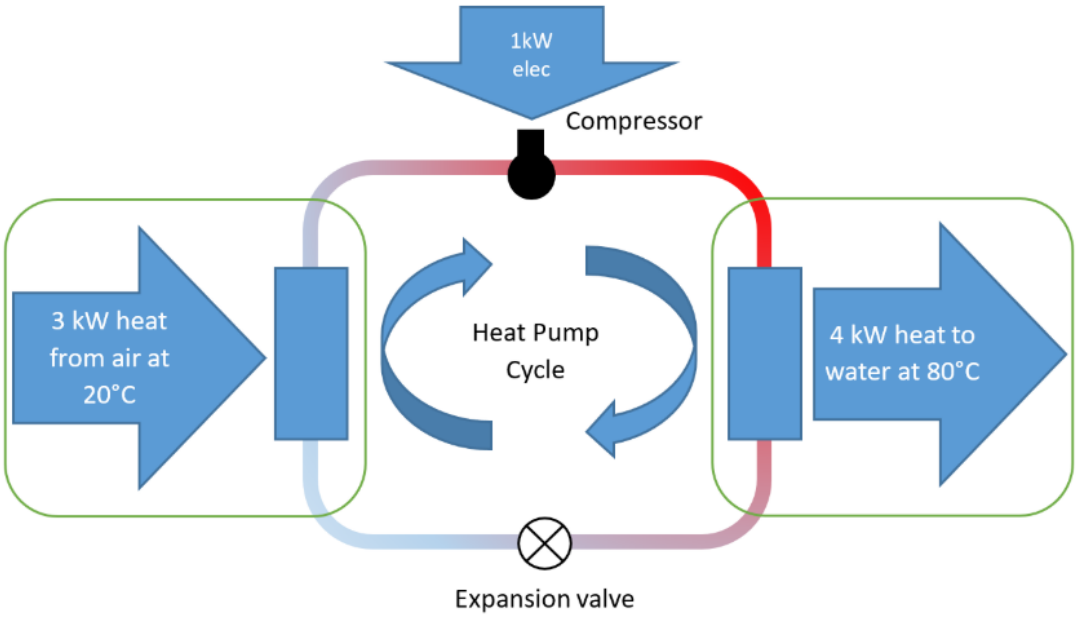

Figure 7 - Example of the energy fluxes in the vapour compression cycle of a heat pump (from [8]).

The efficiency of a heat pump is highly dependent on the temperature difference between the heat source (e.g., outside air, ground, or water) and the desired indoor temperature. The smaller the difference, the more efficient the heat pump, and less electricity is needed to compress the heat carrier fluid (Fig. 7).

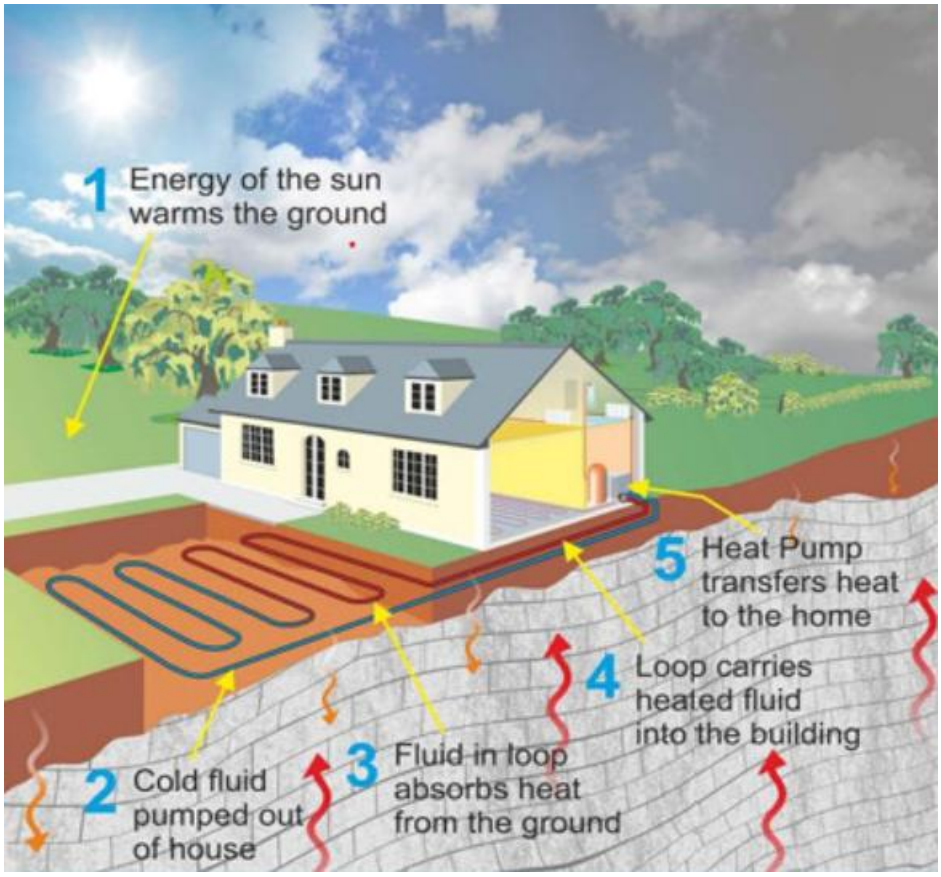

Figure 8 - Ground source heat pump.

The main advantage of Ground Source Heat Pumps (GSHPs) (Fig.8), compared to Air Source Heat Pumps (ASHPs), lies in the relatively stable ground temperature at shallow depths. Unlike air temperature, which varies significantly throughout the year, ground temperature remains nearly constant, being warmer than air in winter and cooler than air in summer.

As illustrated in Fig. 9, temperature variations are significant at the ground surface and within the upper soil layers. However, the amplitude of both seasonal and daily temperature fluctuations decreases progressively with increasing depth. At depths greater than approximately 9–10 m, seasonal temperature variations become negligible, and the ground temperature remains nearly constant throughout the year.

This phenomenon explains common practical observations: for example, underground environments such as subway systems tend to feel cooler in summer and warmer in winter due to the thermal stability of the surrounding ground.

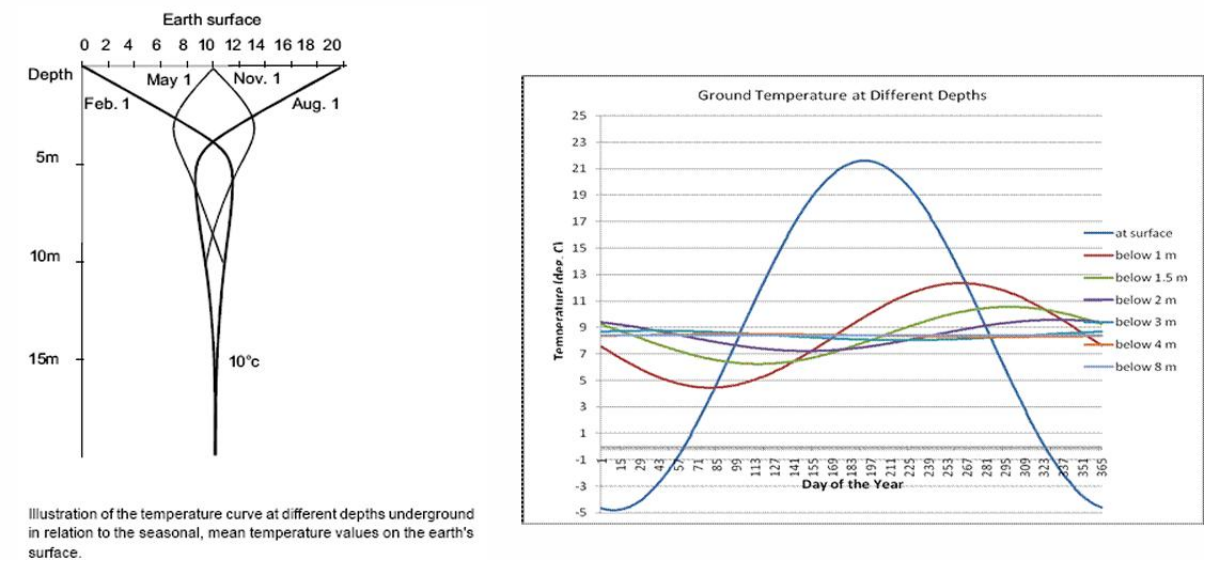

Figure 9 - Ground temperature at different depths (from [19]).

1.4 Closed Loop Systems

Closed loop geothermal systems circulate a heat transfer fluid through a closed network of pipes buried underground. Heat is absorbed from or released to the ground to regulate building indoor temperatures, depending on the operating mode (heating or cooling). The main types of heat exchangers include:

- Geothermal piles and geo structures: Pipes integrated in building foundations (Fig. 10).
- Shallow Horizontal Collectors (SHC): Installed at depths of approximately 1–3 m and available in various configurations, such as coils, linear trenches, and geothermal baskets.
- Borehole Heat Exchangers (BHEs): Pipes in vertical boreholes filled with grout, which are the most used configuration due to its design flexibility, easier management, higher thermal performance compared to geothermal piles and open loop systems, and lower surface area requirements compared to SHC (Figs. 11–12).

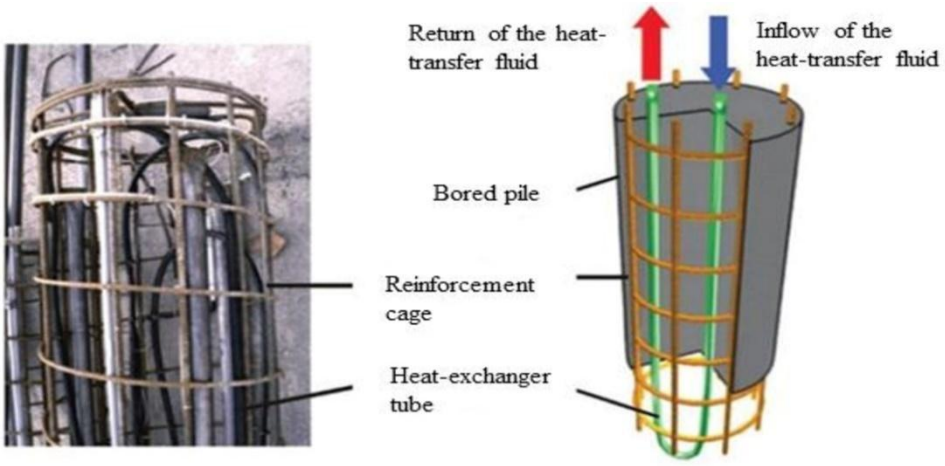

Figure 10 - Geothermal piles and geo structures (from [9]).

Figure 5 - Borehole Heat Exchangers (BHEs) (from [9]).

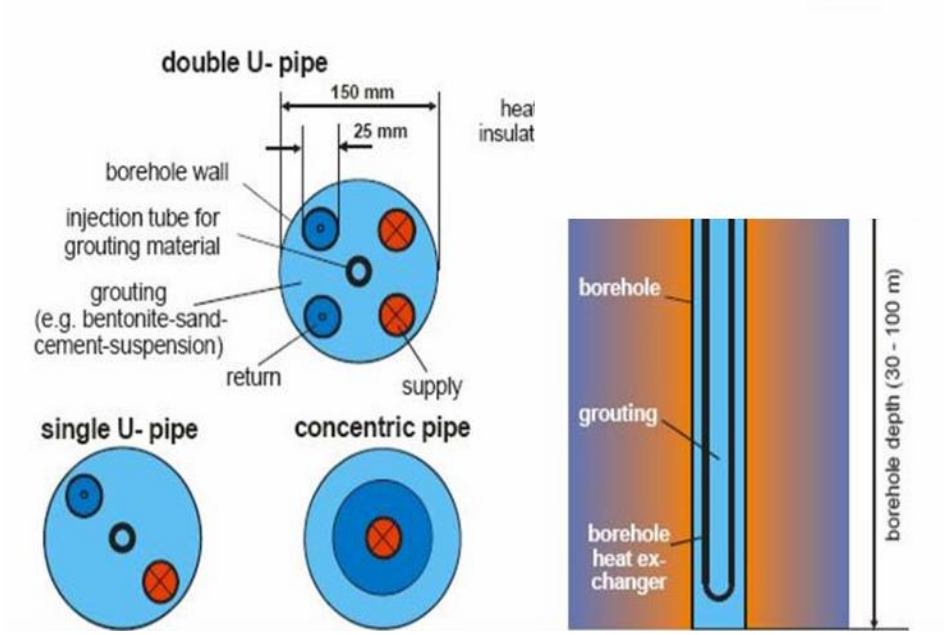

Figure 6 - Borehole Heat Exchangers (BHEs) (from [10].

The heat transfer between the ground and the geothermal circuit is ensured by the grout material, which fills the borehole annulus. Grout is typically a semi-fluid mixture composed of water, Portland cement, bentonite, quartz sand, and specific additives. It serves several functions: sealing the borehole to prevent groundwater mixing, eliminating air gaps (which reduce thermal conductivity), reinforcing structural stability, and enhancing thermal exchange between the borehole and the surrounding ground (typically 2–2.2 W/m·K).

BHE pipes are generally made of high-density polyethylene (HDPE), designed to withstand pressures of 10–16 bar. Considering that hydrostatic pressure increases by approximately 1 bar every 10 m of water column, a 100 m deep borehole requires pipes resistant to at least 10 bar.

Pipe configurations may include single U-tube (1U), double U-tube (2U), or coaxial arrangements. Double U configurations improve heat exchange performance and provide redundancy, ensuring continued operation in case of partial failure.

1.5 Open Loop Systems

An open loop geothermal system exchanges heat directly with groundwater extracted from a nearby aquifer. The pumped water transfers thermal energy to (or from) the indoor heat pump through a heat exchanger.

After the heat exchange process, the groundwater is either re-injected into the same aquifer through a discharge (or reinjection) well located at an appropriate distance from the production well or discharged into a surface water body or an approved drainage system (Fig. 13).

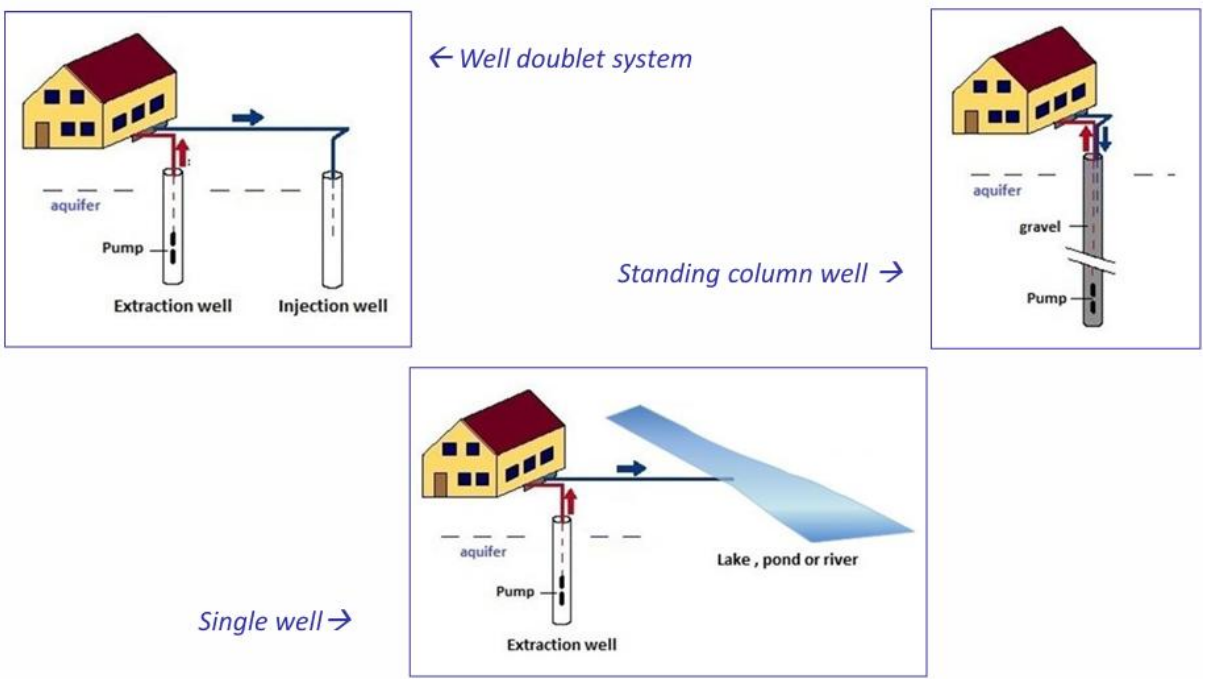

Figure 13 - Open loop system types (from [19]).

There are three different types of open loop systems:

- GWHP with surface discharge: The extracted water is re-injected into the same aquifer but in a surface water body system near the plant (e.g., lake or river). This represents the easier and cheaper way to discharge, as it avoids thermal recycling. However, this application creates a decay of performance and ground water quality.
- GWHP with re-injection: The extraction and re-injection of water is performed in the same aquifer using two or more wells. This is the most common configuration. However, the thermal and hydraulic recycling phenomena must be carefully considered during system design.
- Standing column well: A single vertical well is used for both extraction and reinjection. This configuration is generally less common and may involve greater operational complexity compared to other open-loop systems.

1.5.1 Installation

GWHP systems with re-injection are the most common configuration. In this approach, the waste groundwater is reinjected back to the same aquifer from which it was abstracted. This is advantageous because there is no net abstraction of water from the

aquifer and it will often minimize any risk of ground settlement that may occur in some soils. Such systems typically require at least two wells: an extraction well upstream and an injection well downstream, aligned with the natural groundwater flow.

To construct a groundwater-based open-loop heating or cooling system, a suitable aquifer is required. It must yield enough water to support the required heating or cooling load of the system. The following parameters must then be defined:

- Well depth: This depends on the depth of the aquifer stratum, the groundwater level and, to some extent, the hydraulic conductivity of the aquifer. Wells may range from a few meters in shallow alluvial deposits to several hundred meters in deeper aquifers.
- Well design diameter: This is determined by the yield of the well, which will in turn affect the diameter of the required pump.
- Design yield of the well: This is constrained by the hydraulic properties of the aquifer and by the desired heating or cooling load.
- Aquifer lithology: This is governed by the type of well required, drilling method and the installation cost.

There are a several ways used to drill wells based on wide range of machines and tools:

- Percussion method: Suitable for constructing large diameter wells (more than 1 m), typically limited to shallow depths of approximately 10–20 m.
- Rotary with direct circulation method: Used for small diameter wells without depth limitations.
- Rotary with reverse circulation method: Preferred for large diameters and deep wells.
- Roto-percussion or Downhole (DTH**)** Hammer: Used to drill deep holes in hard rock formations or concrete.

An extraction well is composed of a casing, a screen, a submersible pump and other components (Fig. 14).

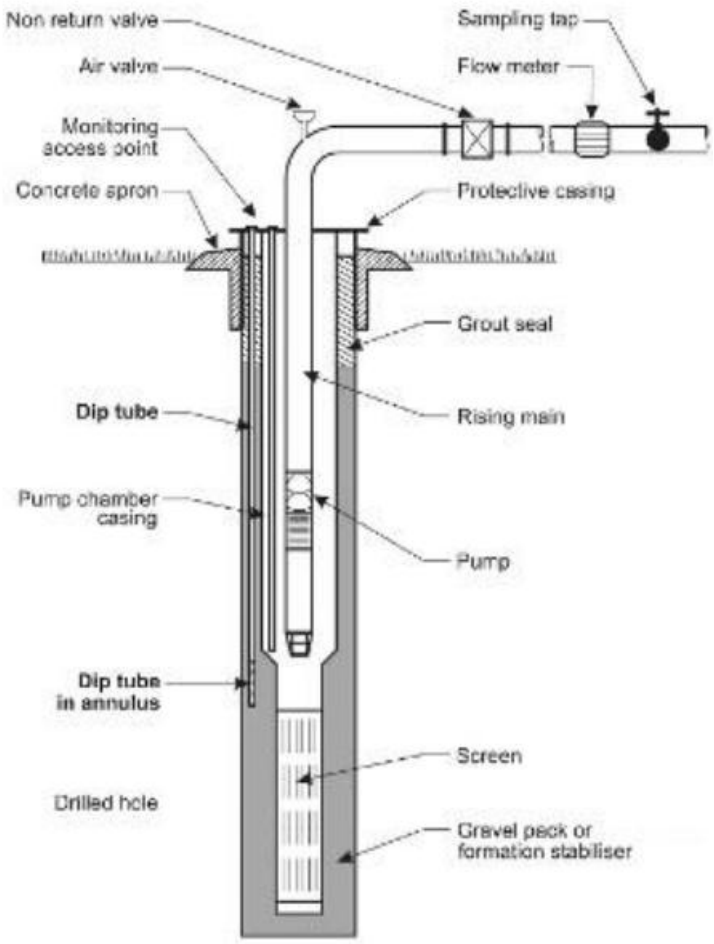

Figure 7 – Scheme of an abstraction water well (from [20]).

1.6.2 Design of of GWHPs

Often, a heat pump is used to provide space heating or active cooling,

The amount of power P [kW] that we can extract from a flow of water is given by:

$$P = (pc)_w \, Q\Delta T_w \tag{1.1}$$

where: Q [m^3/h] is the abstracted flow of water, ΔT_w [K] is the temperature difference between extracted and injected water, $(pc)_w$ is the thermal capacity of water equal to 1.16 $kWh/m^3.K$.

Since $(pc)_w$ is constant, variation in Q or ΔT_w gives a range of thermal power, Q is function of hydraulic properties of the aquifer; if the aquifer is not permeable, draw down in abstraction well is large, and level increase in reinjection well is too large, then we can't sustain Q and

need to increase it. Also, Q is affected by authorization procedures, choosing Q and well diameter available affect Q in urban spaces.

while ΔT_w is function of temperature regulations, variable respect to the analyzed area, and generally ranges between 3 and 5°C.

1.6.3 Thermal and hydraulic recycling

If groundwater is reinjected too close to abstraction well, short-circuiting may occur. In such cases, the thermally altered groundwater (colder in heating mode or warmer in cooling mode) can migrate toward the production well, forming a thermally affected zone commonly referred to as a *thermal plume*.

As a result, the temperature of the extracted groundwater gradually drifts over time, leading to a reduction in system efficiency. This phenomenon is known as thermal and hydraulic recycling (Figs. 15–16).

In cooling mode, the intensity of temperature variations progressively decreases with distance from the reinjection well. This attenuation is due to thermal dispersion within the aquifer and heat conduction through the surrounding geological formations.

The thermal plume generated by the reinjection well typically elongates in the downstream direction, following the natural groundwater flow. If the abstraction well is positioned within the influence zone of this plume, thermal interference may occur.

In heating mode, an increase in the reinjection temperature may lead to a rise in the inlet temperature at the production well. To maintain a constant outlet temperature (T_{out}), the required temperature difference (ΔT) must be preserved. Consequently, the system may require higher pumping rates (Q), which can intensify hydraulic interaction between wells and promote further recycling. In extreme cases, this feedback mechanism may lead to system performance degradation, as described in Eq. (1.1).

To avoid thermal and hydraulic recycling during system design, the minimum distance between abstraction and reinjection wells should satisfy:

$$L > \frac{2Q}{\pi T \mathrm{i}} \tag{1.2}$$

where Q [m³/s] is the hydraulic flow rate, b [m] is the aquifer thickness, K [m/s] is the hydraulic conductivity, L [m] is the distance between wells, i [–] is the hydraulic gradient, and T [m²/s] is the aquifer transmissivity defined as $T = K$b.

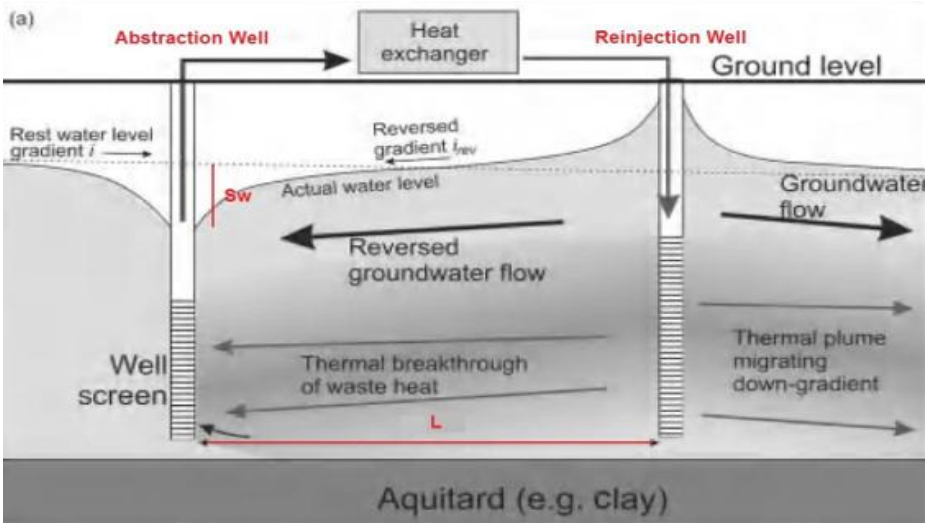

Figure 15 - Thermal and hydraulic recycling (from [19]).

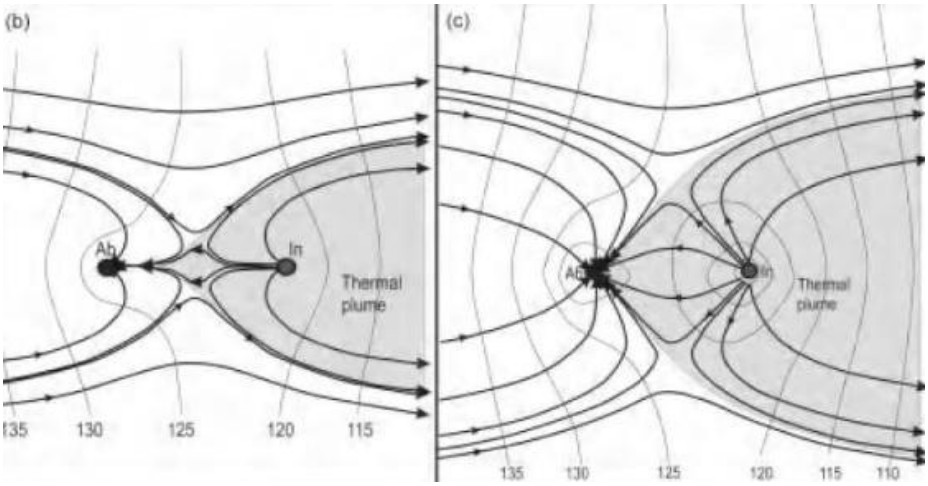

Figure 16 - Thermal and hydraulic recycling (from [19]).

In many practical applications, achieving sufficiently large spacing between abstraction and recharge wells is not feasible; consequently, a certain degree of hydraulic and thermal feedback must be accepted. However, the presence of this risk does not necessarily imply system failure. Such systems can remain sustainable, or at least operate over a long service life, for several reasons. First, thermal breakthrough at the abstraction well does not occur immediately; depending on the hydrological properties of the aquifer, it may take from several days to several months to develop. Furthermore,

only a limited fraction of the water abstracted at the production well may consist of recirculated water originating from the injection well. Finally, in systems characterized by heating demand in winter and cooling demand in summer, reversible operation is possible. This allows partial recovery of the heat rejected during the summer season in the following winter heating period, thereby mitigating the risk of thermal breakthrough and improving the long-term thermal balance of the system.

1.6.4 Advantages of ground water based open loop systems

The system utilizes groundwater, a naturally occurring subsurface medium known for its relatively stable temperatures and high heat capacity. It extracts heat through the forced convection of groundwater, which allows for higher heat extraction per well compared to closed loop systems that rely on subsurface conduction. Interestingly, the quality of the abstracted groundwater is not necessarily a limiting factor; for instance, in scenarios where groundwater is pumped for the remediation of a contaminated site, such as in "pump-and-treat" schemes, thermal energy can be recovered simultaneously during the treatment process. Additionally, these systems can also be based on natural saline groundwaters, particularly in coastal areas.

1.6.5 Disadvantages of ground water based open loop systems

Open loop systems are geology-dependent, necessitating the presence of an underlying aquifer capable of providing a sufficient yield. To ensure optimal performance and sustainability, these systems require extensive design input from a hydrogeologist or groundwater engineer. Additionally, they involve the construction of one or more durable, properly built, and often costly water wells, along with the installation of pumps, monitoring systems, and control mechanisms. These systems generate a discharge flow that must be legally managed and disposed of in accordance with environmental regulations. There is also a risk of fouling or clogging of the heat exchanger, making it essential to monitor and regulate factors such as turbidity, chemistry, microbiology, and pressure within the groundwater circuit. In urban areas, open loop systems face challenges including limited underground space, groundwater contamination, interference between facilities, lengthy permit processes, and competition with alternative energy sources.

2 Description of the case study

2.1 Hydrogeological setting

2.1.1 Topographic Setting

The study area (Città Studi) is located in the Po Plain (Northern Italy), within the Lombardy region, in the eastern sector of Milan (Zone 3), at approximately 45.477° N and 9.231° E (Fig. 17). The district hosts most of the technical and scientific faculties of Politecnico di Milano, as well as several departments of the Università degli Studi di Milano. According to the 2018/2019 academic report, Politecnico di Milano had approximately 49,000 enrolled students across its campuses.

The Milan metropolitan area covers 535 km^2 within the Po Plain in northern Italy, characterized by relatively flat topography, with elevations ranging from 140 m to 99 m above sea level (a.s.l.).

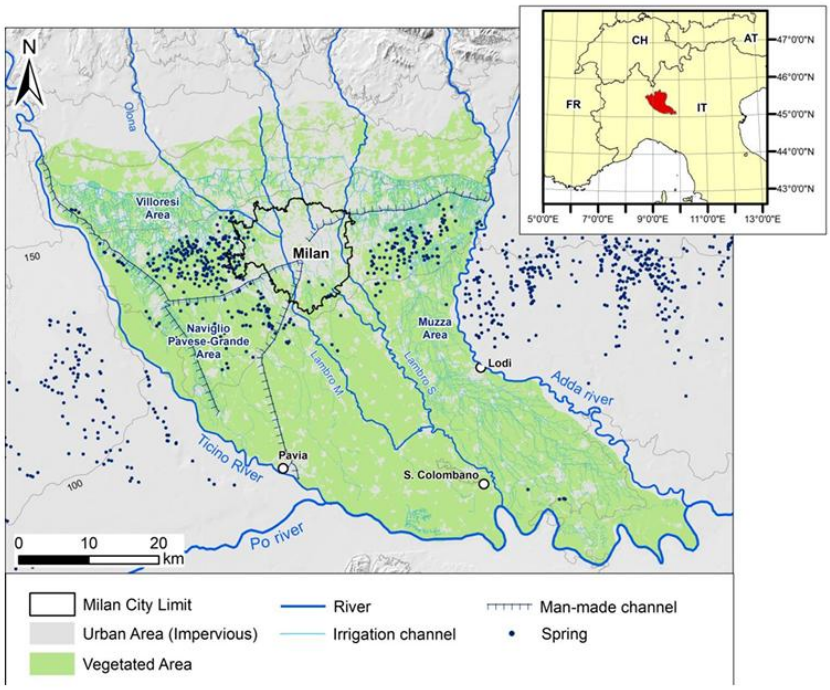

Figure 17 - Map of the Lombardy region showing the Milan city area, and the hydrological network: rivers, springs, irrigation networks, and man-made canals (from [17]).

2.1.2 Climate Setting

The Milan metropolitan area is located relatively far from the sea and is characterized by a humid climate with some continental features, typical of many inland plains in northern Italy. Summers are generally hot, humid, and muggy, while winters are cold and wet.

The average annual precipitation is approximately 900 mm, with most rainfall occurring during spring and autumn. The mean annual air temperature is about 13 °C, with average daily maximum temperatures reaching approximately 24 °C during summer.

2.1.3 Geological and hydrogeological settings

The city of Milan lies within the Po Plain, which represents the peripheral foreland basin of the Alps. The subsurface consists of a sedimentary aquifer system composed of three main depositional sequences, from bottom to top (Fig. 18):

- Deep confined aquifer (C): Aquifer Group C, consists of sandy lenses within clay and silt units.
- Semi-confined aquifer (SC): Known as Aquifer Group B, consists of sands and sandy gravels with a thickness in the range between 50 m and 150 m.
- Unconfined aquifer (P): Also known as Aquifer Group A or together with the semi-confined aquifer, consists mainly of gravel with a sandy matrix. The aquifer, with a thickness in the range between 20 m and 100 m.

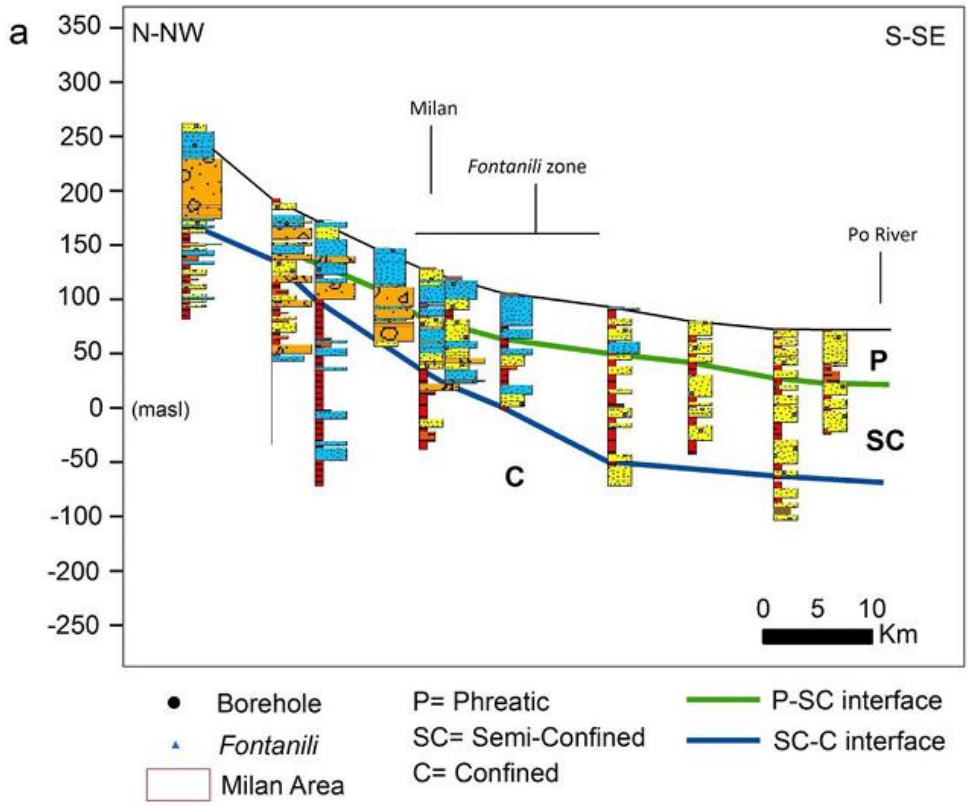

Figure 8 - Simplified cross-section profile showing the investigated aquifers (source: Region Lombardy and ENI 2002).

2.2 Monitoring groundwater level in Milan.

The groundwater monitoring system is designed to collect long-term data on aquifer properties to support the study and management of water resources and their evolution over time. Key monitored parameters include groundwater levels, temperature, and quality. This process relies on electronic devices known as dataloggers, which provide accurate and continuous measurements at specific time intervals.

Regularly tracking groundwater levels and quality is essential for ensuring resource availability and sustainable management (Fig. 19).

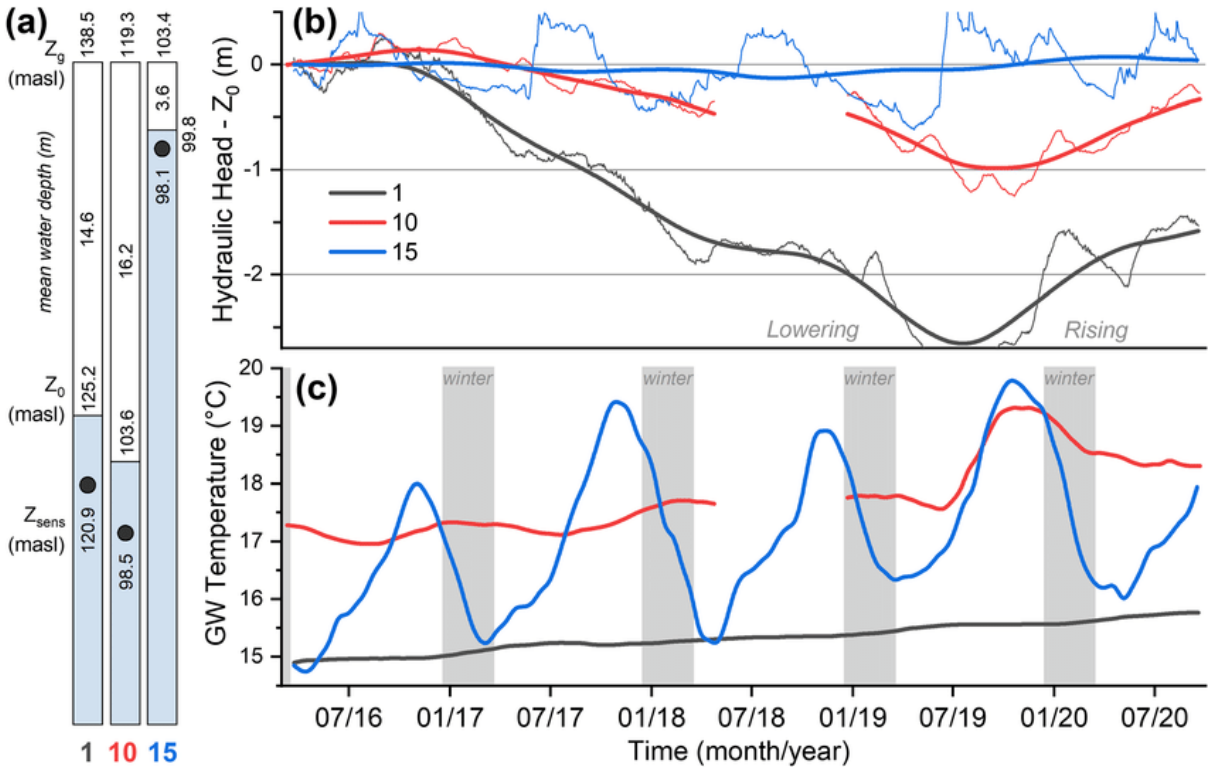

Figure 19 - Time series at three selected locations for the period 2016-2020: a ground elevation (Z g), water-table depth, hydraulic head as on March 2016 (Z 0) and sensor (black dots) elevation (from [17]).

2.2.1 Evolution of groundwater withdrawals and levels

Groundwater levels in the Milan area can be analysed in relation to Italy's socio-economic developments. Historical pumping data are available for hundreds of wells, with depths ranging from 40 to 150 m, within the city (Fig. 20). Additionally, several groundwater monitoring networks have been collecting data in the study area since the early 20th century.

Groundwater abstraction rates in the Milan area have fluctuated over time, reaching a peak of approximately 700 × 10^6 m^3/year in the mid-1970s before declining to around 230 × 10^6 m^3/year in recent years. Map presents groundwater level time-series data (1950–2016) for 20 monitoring points across the Milan Metropolitan area, alongside historical pumping rates.

Following post-war reconstruction and the economic boom (1950–1975), extensive groundwater extraction led to a 10–15 m decline in the water table of the unconfined aquifer. During the oil crisis (1975–1980), a sharp reduction in pumping resulted in a rapid

groundwater rise of 7–8 m. After a stable period (1980–1985), groundwater abstraction decreased again due to the European Monetary System crisis and economic downturn. Since the 1990s, groundwater levels have been rising, with a maximum rate of 1 m/year between 2008 and 2014. The aquifer system is largely influenced by the hydrographic network, maintaining a shallow water table (Fig. 21).

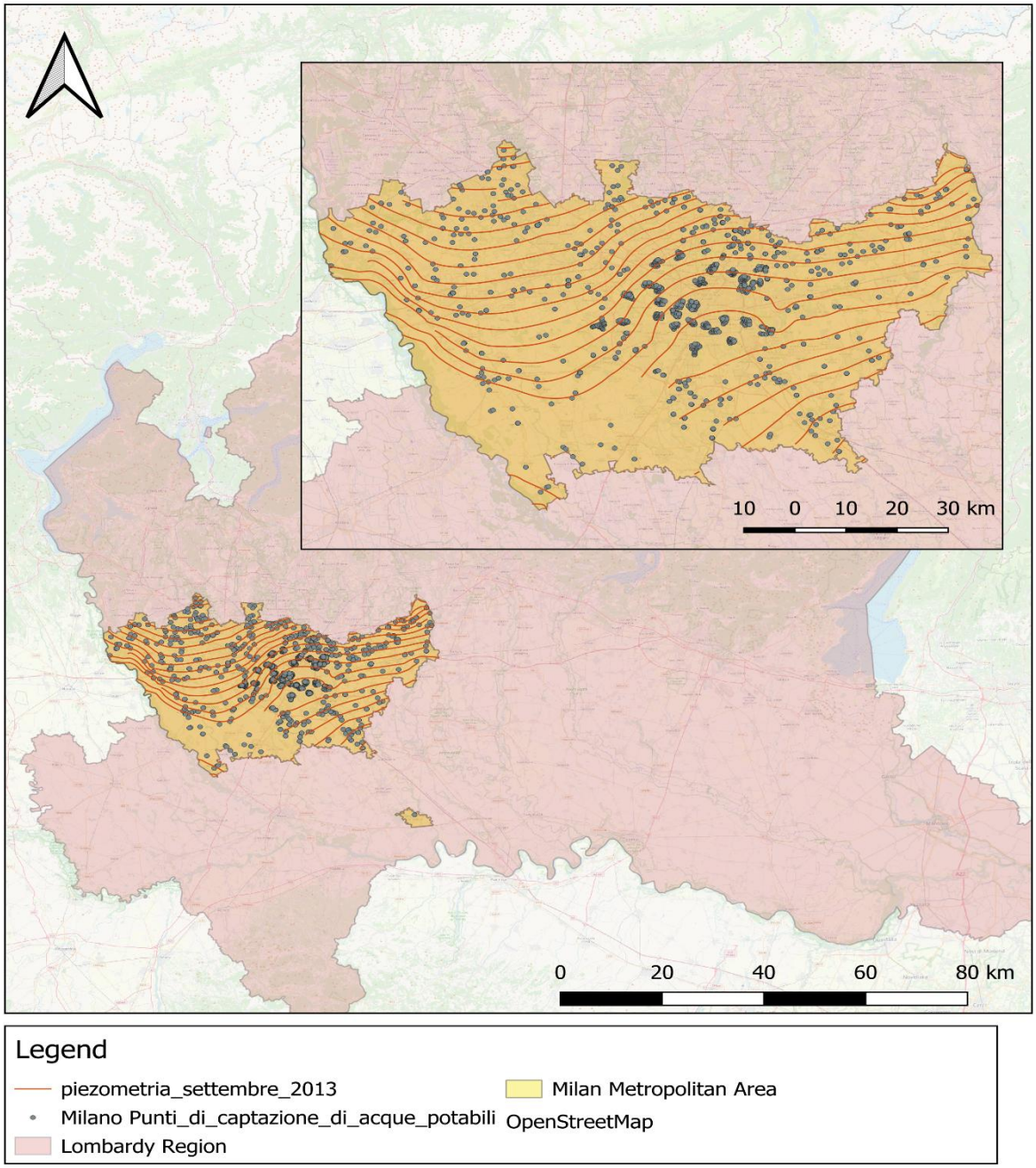

Figure 20 - Piezometric surface of the Milan Metropolitan Area in September 2013 (QGIS).

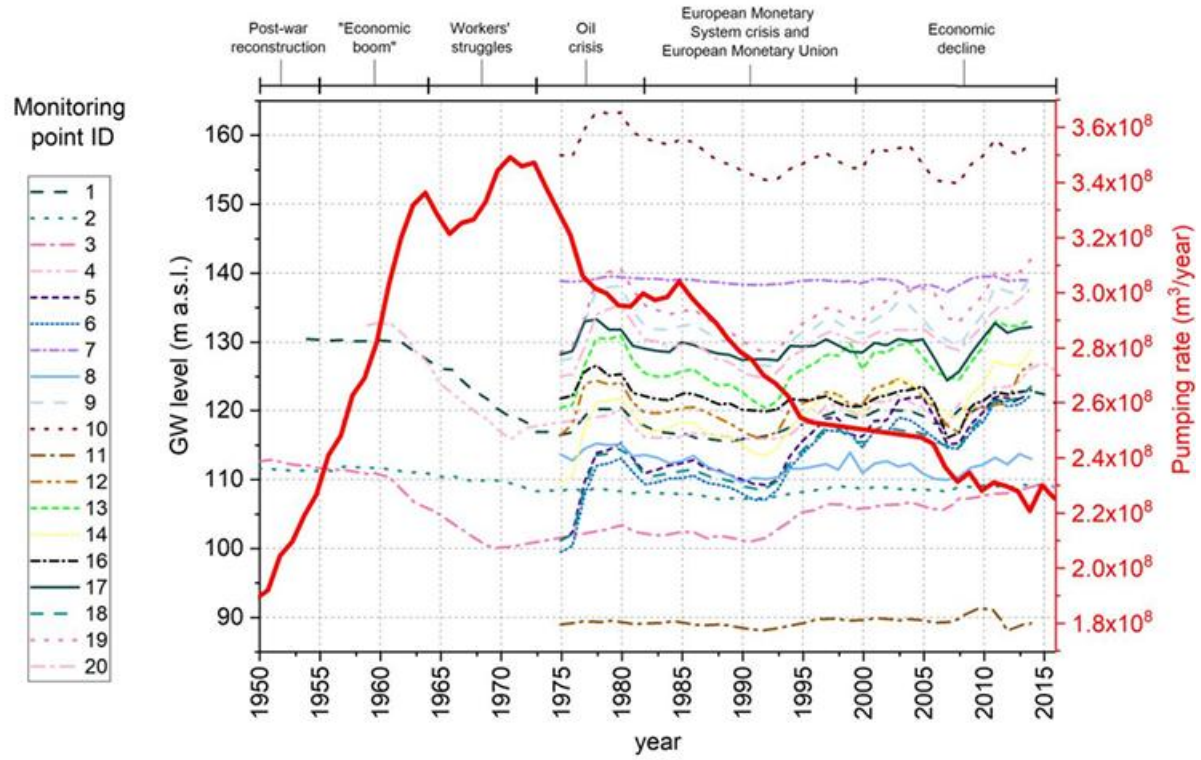

Figure 21 - Historical (i.e. 1950-2016) monitoring data of groundwater levels for the unconfined aquifer, and total groundwater abstraction rate (red line) for the wells within Milan area (from [17]).

2.2.2 Groundwater interaction with underground structures

Historically, the city was interwoven with a dense network of natural and artificial channels serving various purposes, including military defence (during Roman times), irrigation, livestock farming, power generation, laundry washing, sewage collection, and recreational activities.

However, between the late 19th and early 20th centuries, many of these channels were covered and buried, disrupting the hydraulic continuity of the network and limiting surface water drainage.

Initially, this did not create major issues, largely due to the presence of large factories in northern Milan. From the early 1960s to the early 1990s, these industries pumped vast amounts of groundwater, up to 140,000 m^3/day, causing significant water table drawdown. However, with the closure of many factories in the early 1990s due to deindustrialization process, this trend reversed and groundwater levels began to rise.

These fluctuations in groundwater levels triggered land subsidence phenomena and contaminant inflow, followed by a phase characterized by increasing interaction between

rising groundwater and underground structures. The reduction in groundwater withdrawals created hydrogeological risks for existing underground infrastructures such as metro tunnels, stations, and deep foundations.

Several actions are necessary to accomplish this task, namely, i) analyzing monitoring data to reconstruct the regional trends of the water table, ii) calibrating a 3D numerical model of groundwater flow, and iii) simulating various scenarios for the evolution of the aquifer system and assessing their potential impacts, such as thermal effects on underground infrastructures.

3 Subsurface flow and heat transport modelling

This study analyses subsurface groundwater flow and heat transport through the development of a numerical model simulating the operation of an open-loop geothermal system using FEFLOW 8.1 (Finite Element Subsurface Flow and Transport System), a widely used groundwater modelling software.

FEFLOW simulates groundwater movement in aquifers while accounting for processes such as pumping, recharge, and natural flow. The software can also model temperature variations and heat transport in the subsurface. In addition, it allows the simulation of contaminant transport in groundwater, supporting risk assessment and the design of remediation strategies. These capabilities make it a valuable tool for designing monitoring networks, evaluating infrastructure impacts on water resources, and supporting sustainable groundwater management.

FEFLOW is based on the finite element method, which enables accurate representation of complex geological structures and groundwater flow systems, particularly in irregular domains.

In this section, the domain of interest is defined, with particular attention given to other geothermal systems in the area that may influence groundwater flow and the thermal plume. Additionally, setting boundary conditions, aquifer parameters, and the plant's operational cycle will be taken into consideration to simulate the thermal plume transport.

The model results help to understand groundwater flow and its temporal evolution, analyse heat transport, improve system design (e.g., well placement and remediation plans), forecast future scenarios, and test different management strategies.

3.1 Development of the numerical model

3.1.1 Conceptual model

The conceptual model represents the first and most important step in groundwater or geothermal simulations using FEFLOW or other hydrogeological modelling software. It provides a simplified representation of the subsurface system and describes the main processes controlling groundwater flow and heat transport.

It includes:

- Model domain: the area to be simulated (e.g., a portion of the Milan metropolitan area influenced by geothermal installations).
- Aquifer structure: the number of layers, the type of soil or rock units, and their thicknesses. Milan area is characterized by two main hydrogeological formations. The shallow aquifer consists mainly of gravel with a sandy matrix and has a thickness ranging between 20 m and 100 m. This upper layer is more permeable, while deeper layers tend to contain higher silt content. In this study, the numerical model focuses on the shallow aquifer, which is considered as the lower boundary of the model domain.

The domain of interest, shown in Fig. 22, has an approximately trapezoidal shape, is oriented from north to south according to the adopted reference system and is bounded by two iso-piezometric lines representing groundwater levels of 115 m and 95 m, respectively. The study area includes the Città Studi district, where the open-loop geothermal system under investigation is located. In addition, the domain includes other geothermal installations and piezometers distributed across Milan, which are used as monitoring points in the subsequent analysis.

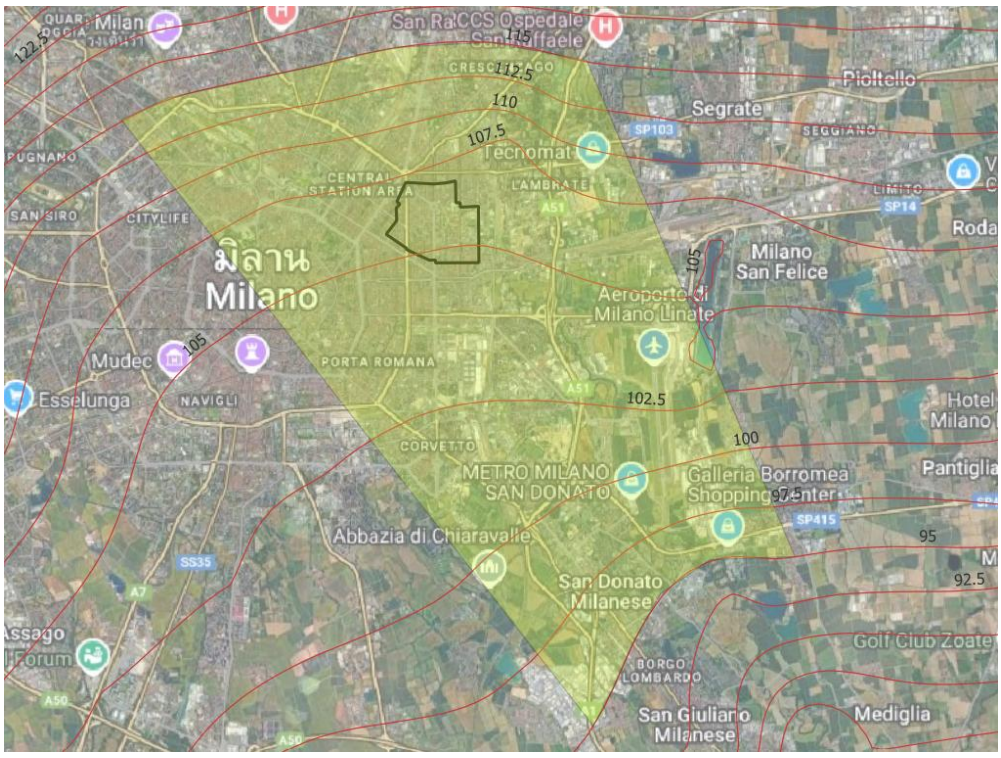

Figure 22 -Modelling domain.

The model includes 22 wells (11 abstraction wells and 11 injection wells) distributed across the study area. Abstraction wells are located upstream, while injection wells are positioned downstream.

The well locations were selected in accessible urban zones, such as gardens, public squares and wide streets to facilitate drilling operations and pipeline installation, as shown in Fig. 23.

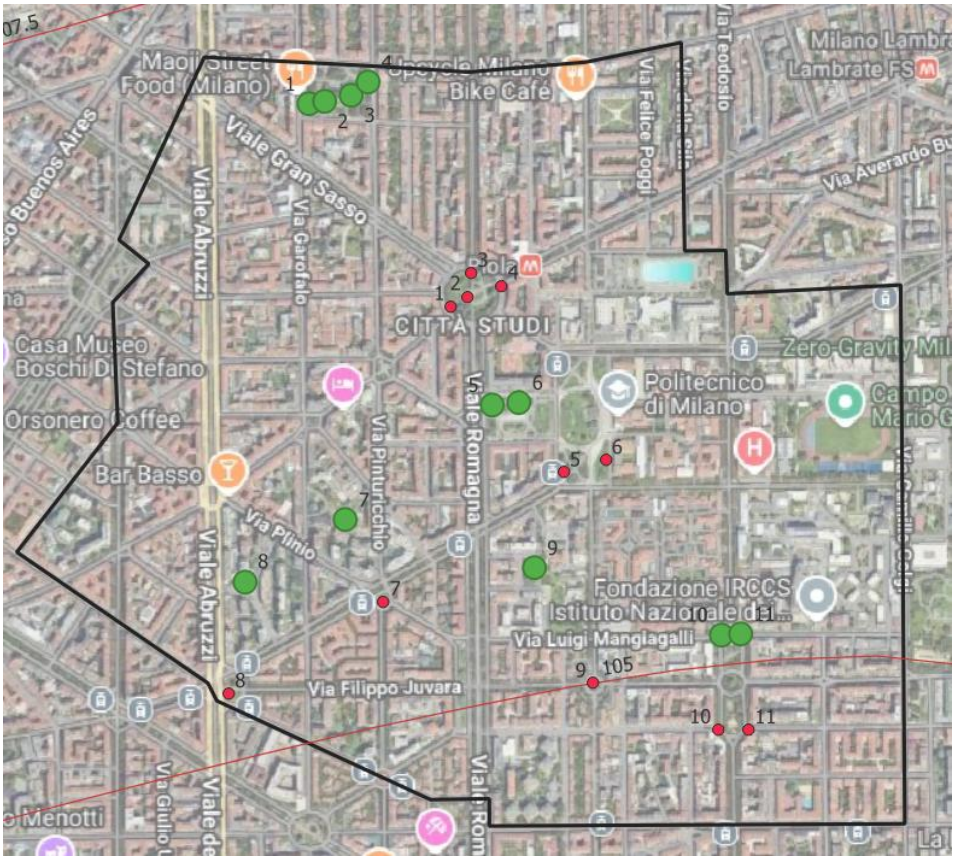

Figure 23 -Abstraction and injection wells within the studies city.

3.1.2 Generating the mesh

In FEFLOW, the mesh is generated as a finite number of geometric elements defined by nodes and connecting lines, forming a two-dimensional mesh. The super-element mesh includes the polygon representing the model domain boundaries, the points representing well locations, and additional points around each well according to the BHE node rule. This mesh serves as the basis for building the numerical model, including the representation of plant components, aquifer properties, boundary conditions, and other relevant features. Before generating the mesh in FEFLOW, the well locations must be

defined, and six additional nodes must be added around each well according to the BHE node rule (Fig. 24).

The computational domain was discretised using a triangular finite-element mesh with three nodes per element. The final mesh comprises 78,034 elements and 39,072 nodes (Fig 25).

A local mesh refinement strategy was applied around the borehole heat exchangers (BHEs) to improve numerical accuracy in regions with high hydraulic and thermal gradients. The element size was progressively reduced in the vicinity of the wells to better capture temperature and pressure variations, while a coarser mesh was maintained in regions far from the wells to optimise computational efficiency.

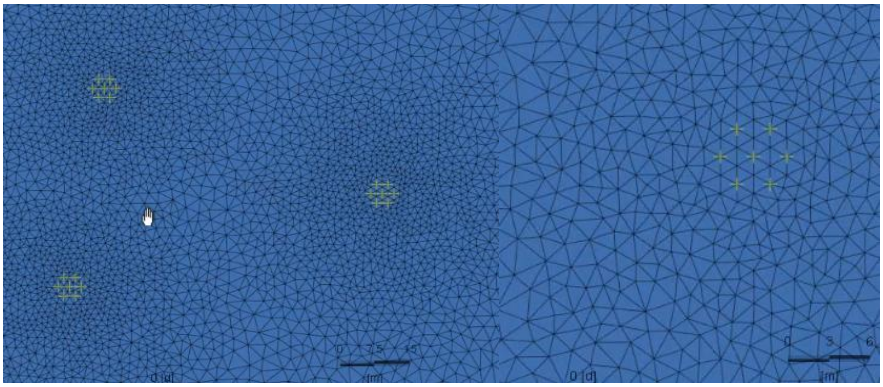

Figure 24 - BHE node rule.

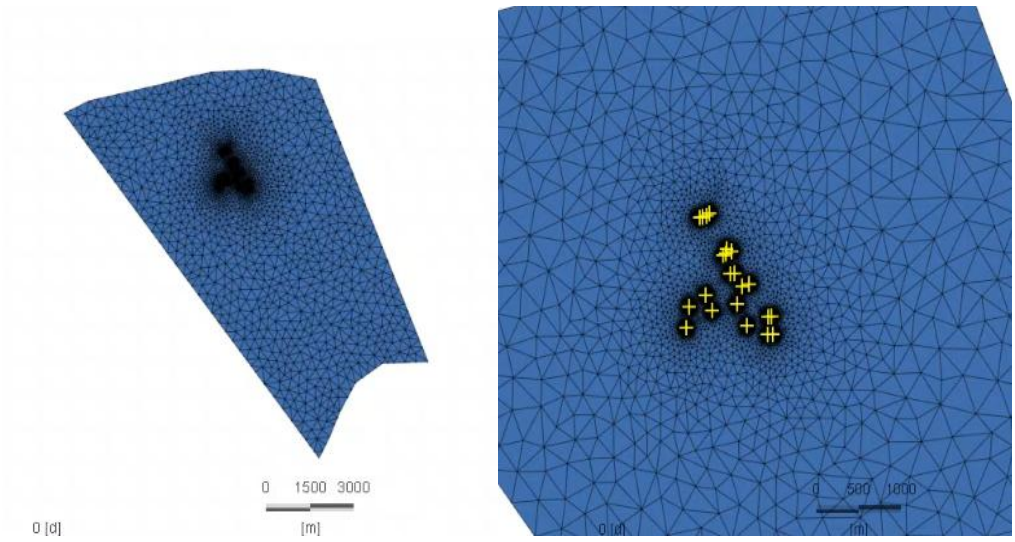

Figure 25 - Mesh.

3.1.3 Smoothing the mesh

The quality and regularity of the mesh significantly influence numerical accuracy and computational stability. Highly irregular elements may introduce numerical distortion and affect convergence behaviour. Therefore, a 2D mesh smoothing procedure was applied to improve element regularity and enhance symmetry within the triangular discretization (Fig. 27).

The smoothing process aimed to reduce element distortion and increase the proportion of near-equilateral triangles, thereby improving solution stability without altering the overall mesh density.

The effectiveness of the smoothing procedure was evaluated by analysing the distribution of maximum internal triangle angles before and after smoothing (Fig. 26). A narrower angle distribution and fewer extreme values indicate improved mesh quality.

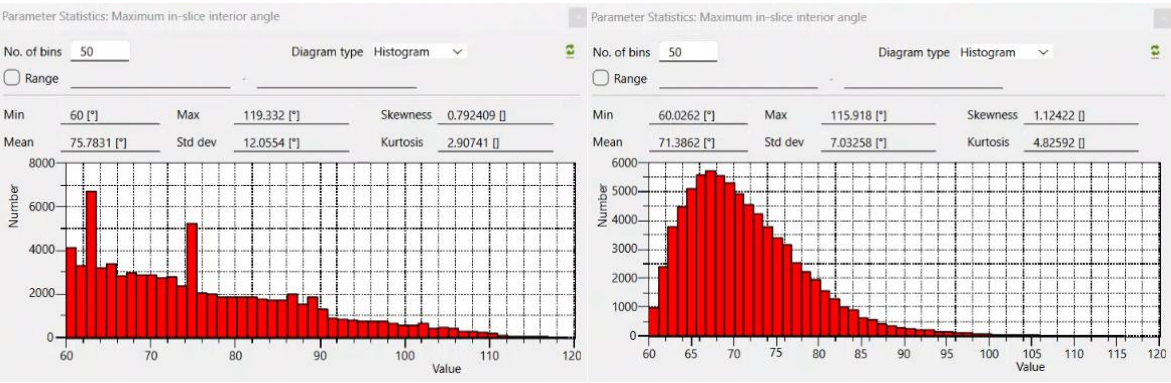

Figure 26 - Distribution of maximum internal angles of triangles before and after smoothing.

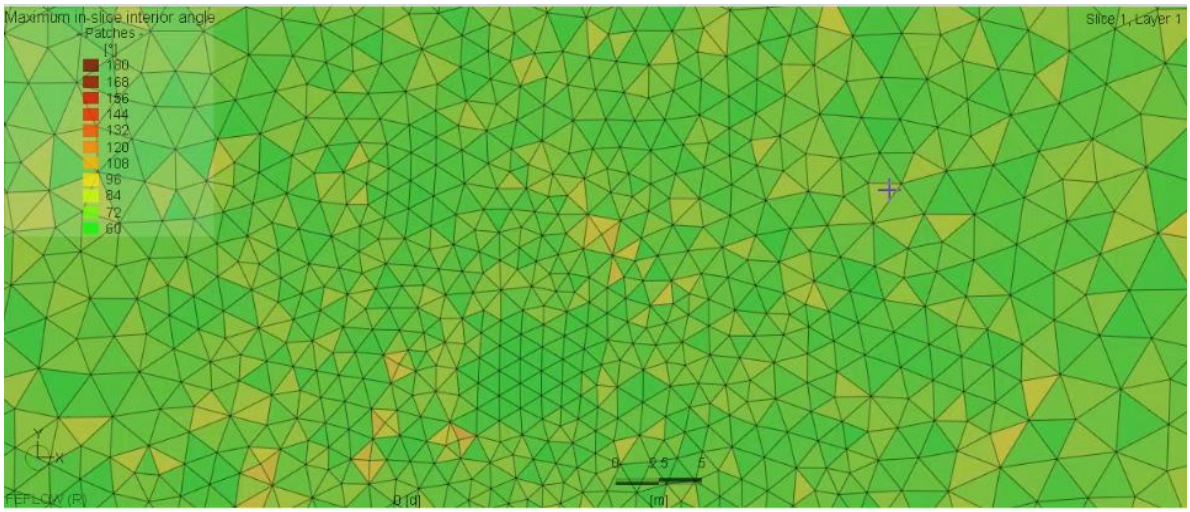

Figure 27 - Smoothed triangular mesh used in the numerical model.

3.1.4 Creating the 3D model

To convert the model from 2D to 3D, the spatial elevation of the domain must be defined. The elevation values (above mean sea level) were assigned to the northern and southern boundaries of the model domain according to the real topographic data obtained from the Digital Elevation Model (DEM) of the Lombardy region. An elevation value of approximately 120 m a.s.l. was assigned to the nodes located along the domain boundaries, as shown in Fig. 28.

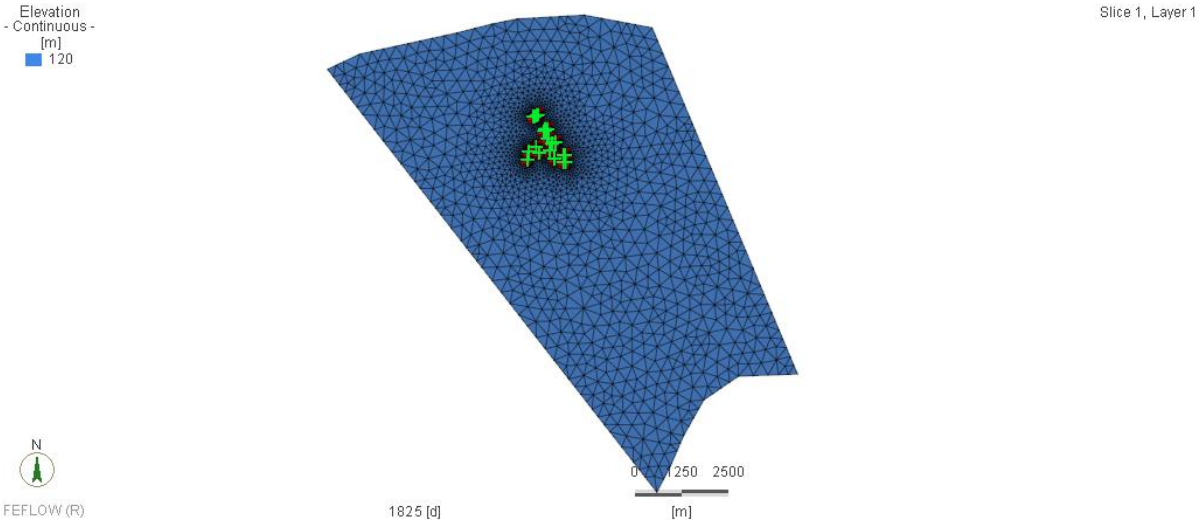

Figure 28 -Elevation Model.

To accurately represent the subsurface geological conditions, the vertical domain was discretised into four geological layers subdivided into five computational slices.

The upper boundary of the model was defined at an elevation of 120 m a.s.l., while the lower boundary was set at 0 m a.s.l. Intermediate slice elevations (90, 60, and 30 m a.s.l.) were automatically generated by the software, ensuring consistent vertical discretisation.

This vertical discretisation was designed to realistically reproduce the subsurface stratigraphy and allow the assignment of distinct hydrogeological and geothermal properties to each layer.

Slice 1 corresponds to the ground surface, whereas Slice 5 defines the fixed impermeable bottom boundary. Slices 2,3 and 4 represent the active aquifer zone, including both the groundwater table and the screened intervals of the wells.

Below Slice 4, an aquiclude layer is defined as an impermeable formation that restricts groundwater flow, with an estimated thickness of approximately 50 m. The three-dimensional configuration and slice distribution are illustrated in Fig. 29.

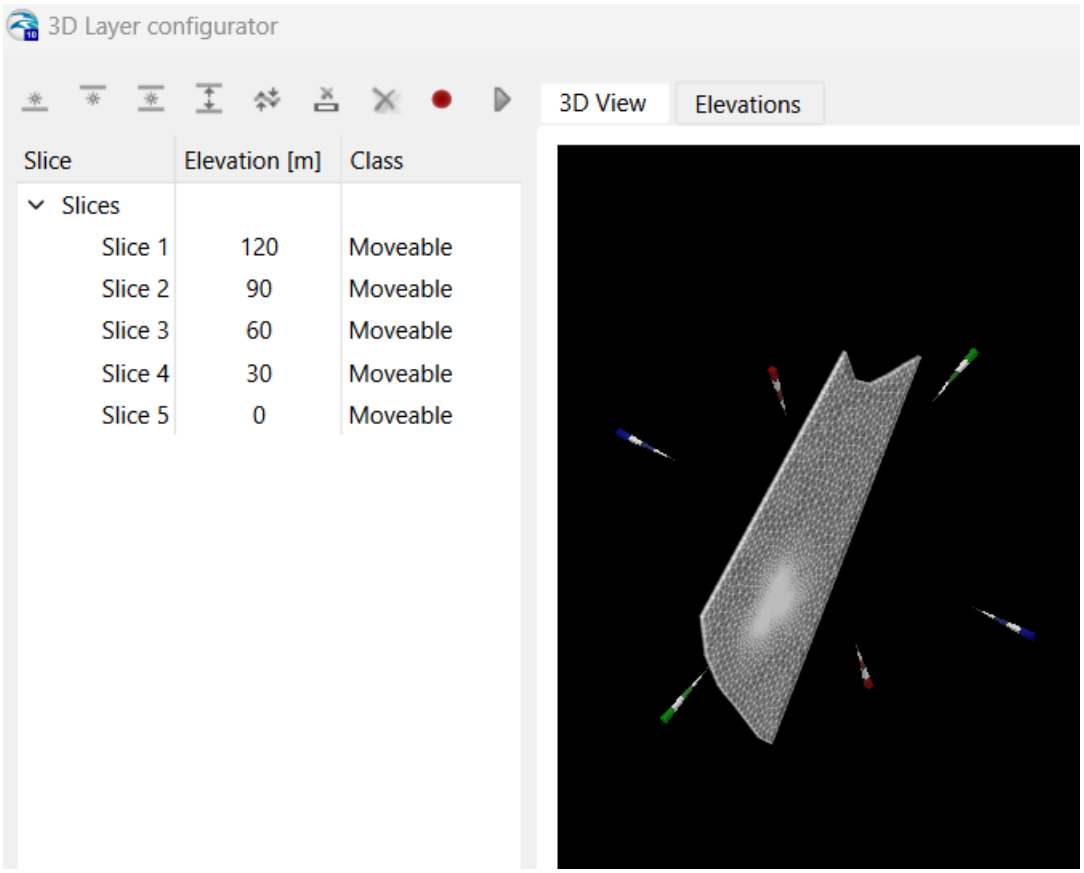

Figure 29 -3D configuration, distribution of slices.

3.1.5 Boundary and initial conditions

In FEFLOW, boundary conditions (BCs) are essential elements that govern the model's behaviour across both space and time. They ensure that the numerical simulation accurately represents the real hydrogeological system. BCs define how the model domain interacts with its surroundings by specifying the external constraints of the model, which control groundwater flow within the system. If these conditions are incorrectly defined, the model may produce unrealistic results, particularly in terms of hydraulic head distribution.

Initial conditions (ICs) define the starting state of the system at the beginning of simulation. These include:

- Initial hydraulic head distribution: representing the spatial distribution of groundwater head (piezometric elevation) at the beginning of the simulation.
- Initial temperature field: representing the subsurface temperature distribution at t = 0.

These conditions are crucial for establishing a baseline from which the model can assess changes over time. Accurate ICs ensure that the simulation results are reliable and reflective.

Flow boundary conditions were defined by imposing fixed hydraulic head values at the upstream and downstream boundaries, as follows:

- Northern Boundary: 110 m.
- Southern Boundary: 95 m.

These conditions were determined based on the piezometric distribution. Using linear interpolation, the software computes the average hydraulic head across the entire domain, resulting the hydraulic head field (Fig. 30).

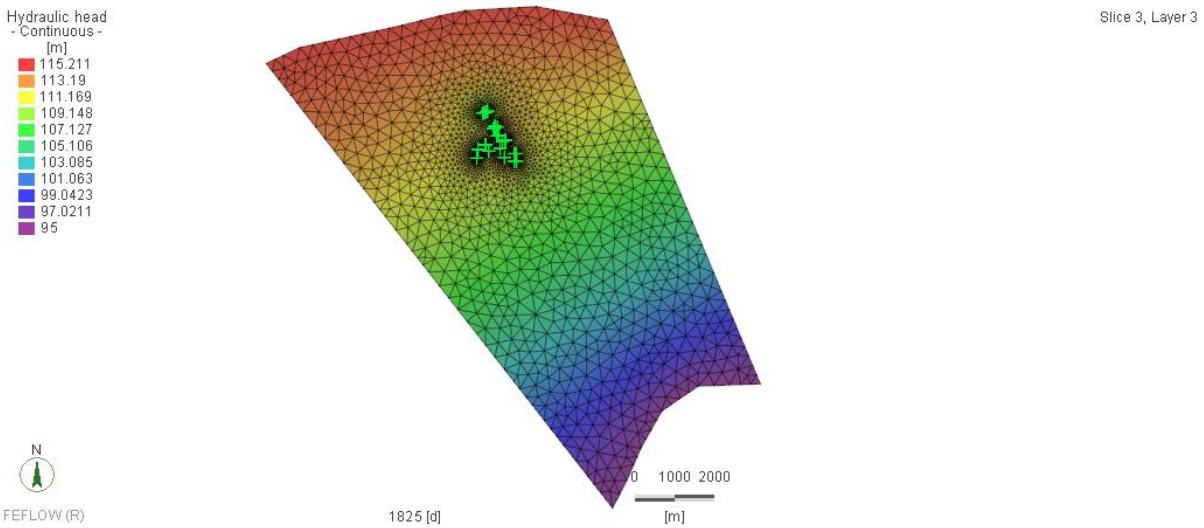

Figure 30 - Hydraulic head distribution.

Similarly, a temperature boundary condition was assigned at the upstream boundary (left border), while the initial temperature of the domain was set to 15 °C. Using linear interpolation, FEFLOW computes the temperature distribution across the entire model domain, resulting in the temperature field shown in Fig. 31.

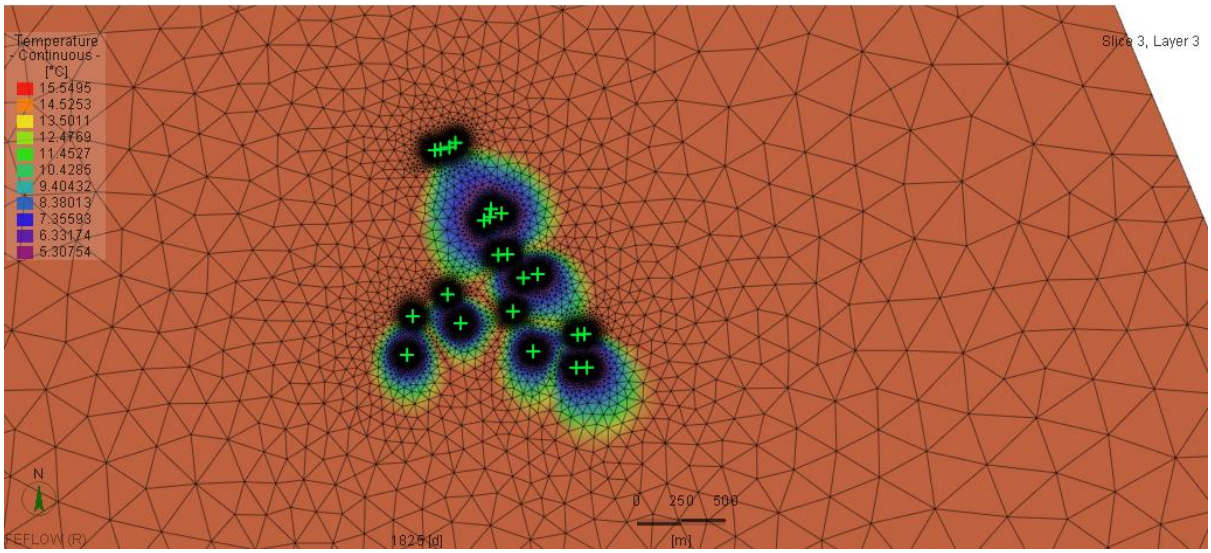

Figure 31 - Temperature distribution.

3.1.6 Time series ID

Assigning time series is essential to represent temporal variations in time-dependent boundary conditions and operational parameters, such as pumping rates, injection rates, and temperature changes. This enables realistic simulation of transient groundwater behaviour, capturing daily and seasonal fluctuations in hydraulic head and temperature.

The time series are defined as follows:

- Flow rate is prescribed using paired values of time (days) and discharge (L/s).
- Temperature is prescribed using paired values of time (days) and temperature (C°).
- Both time series datasets represent the operational cycle of the geothermal system and are implemented in cyclic time mode using a linear interpolation curve.

Each time series is assigned a unique identification number (ID) to ensure correct recognition and parameter referencing within the software.

Negative values are used to denote re-injected groundwater and temperature difference between heating and cooling mode.

FEFLOW uses linear interpolation to automatically generate intermediate values between defined time steps, ensuring smooth and continuous transitions between successive data points. At each computational time step, the software retrieves the corresponding value from the assigned time series and applies it to the relevant nodes or

elements.

This approach enables dynamic adjustment of hydraulic and thermal stresses under temporally varying boundary conditions (Figs. 32–34).

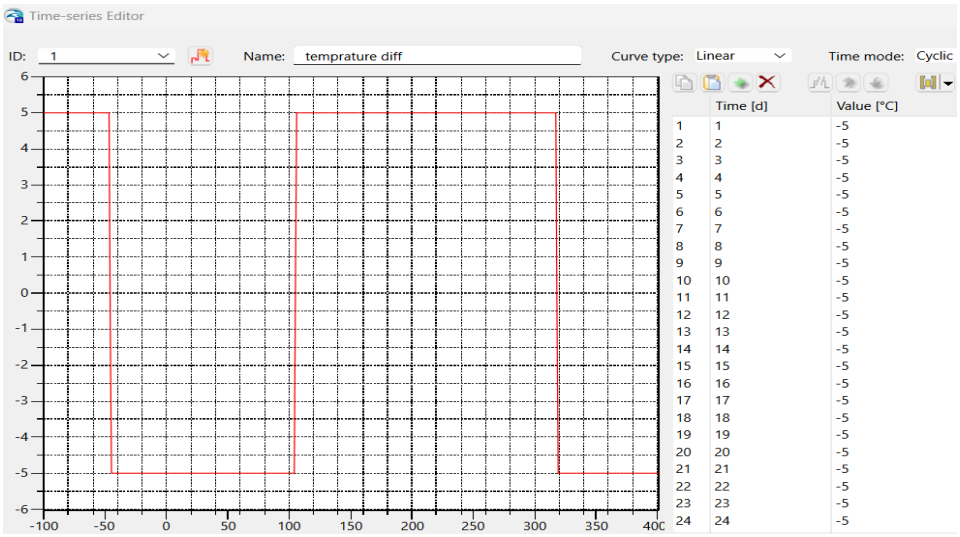

Figure 32 - Time series of the cyclic temperature difference applied.

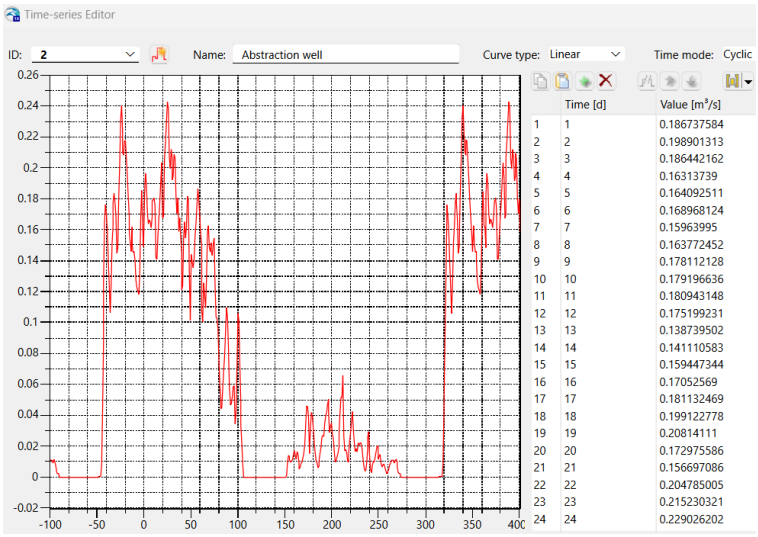

Figure 33 - Time series of the cyclic flow rate extraction.

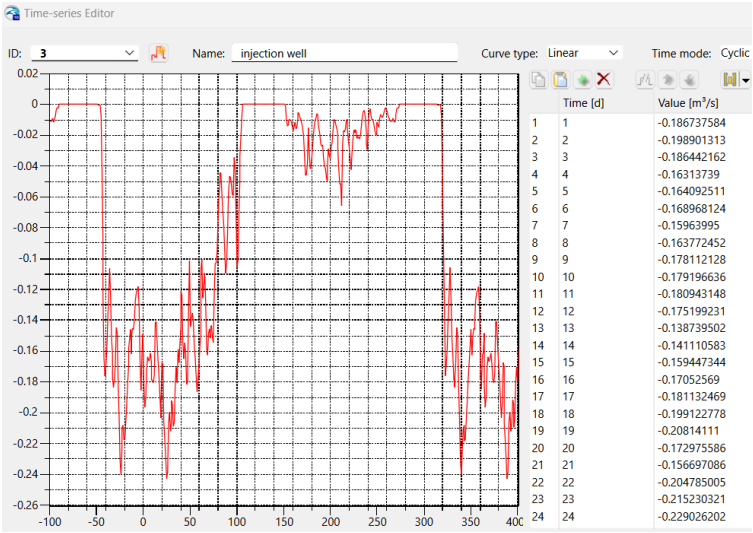

Figure 34 - Time series of the cyclic flow rate injection.

3.1.7 Assigning hydraulic conductivity

Hydraulic conductivity (K) is a key parameter in FEFLOW that directly impacts groundwater flow, hydraulic gradients, and heat transport. Assignment of realistic K values is vital to simulate and understand subsurface processes effectively, Different soil and rock layers (e.g., sand, clay, limestone) have different conductivities.

The following hydraulic conductivity values were assigned: the shallow aquifer (layers1 and 2) at K = 10^{-3} m/s (≈ 86.4 m/day) (Fig. 35), whereas deeper layers (aquiclude, layers 3 and 4) at K = 10^{-8} m/s (≈ 0.000864 m/day) (Fig. 36), considering the anisotropy of the hydrogeological formation.

Furthermore, the porosity of the hydrogeological formation was set to 0.3.

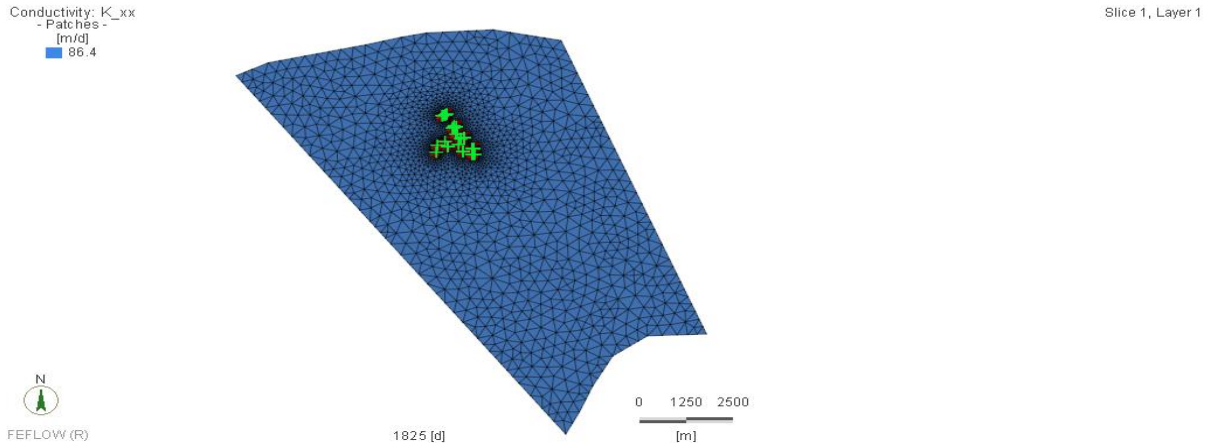

Figure 35 - Hydraulic conductivity distribution layer 1.

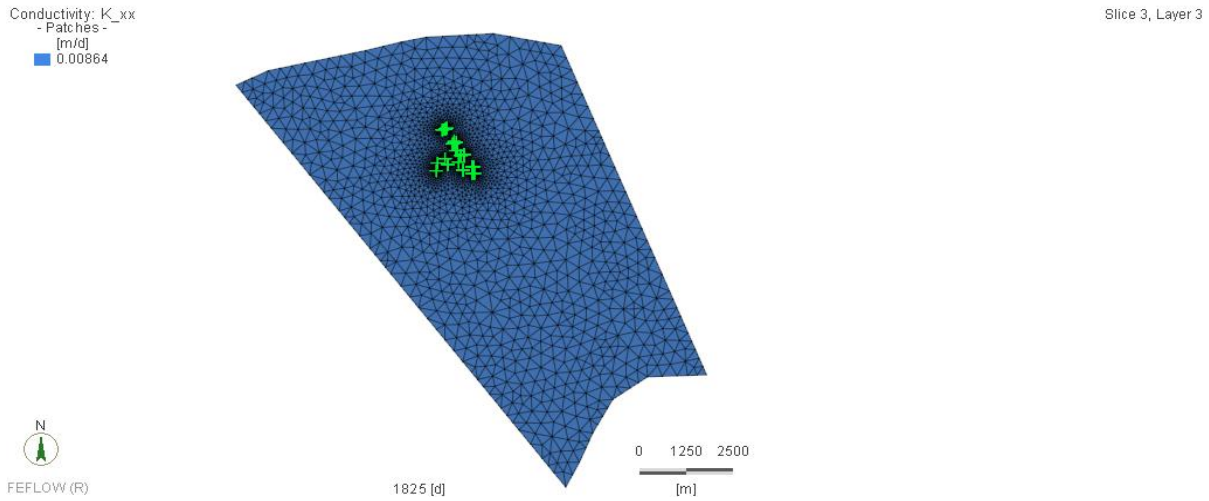

Figure 36 - Hydraulic conductivity distribution layer 3.

3.1.8 Setting the open loop system

Once the aquifer parameters such as hydraulic conductivity and porosity are defined, it is essential to establish the open loop geothermal system configuration in the model. The open loop system allows linking aquifer behaviour with system performance (wells), in terms of groundwater extraction, thermal exchange and reinjection which allow for assigning flow rates, tracking thermal plumes, assessing hydraulic and thermal interference and monitoring long term system performance.

The software identifies the flow path between the extraction and injection wells by assigning a specific value to each well node, distinguishing them from the other nodes that compose the mesh. In this way, during the simulation, a hydraulic connection is established from the 11 extraction wells toward the 11 downstream injection wells.

This configuration enables the model to simulate the resulting thermal plume, which develops as a function of the imposed boundary conditions and the hydraulic and thermal properties of the domain, as shown in Fig. 37.

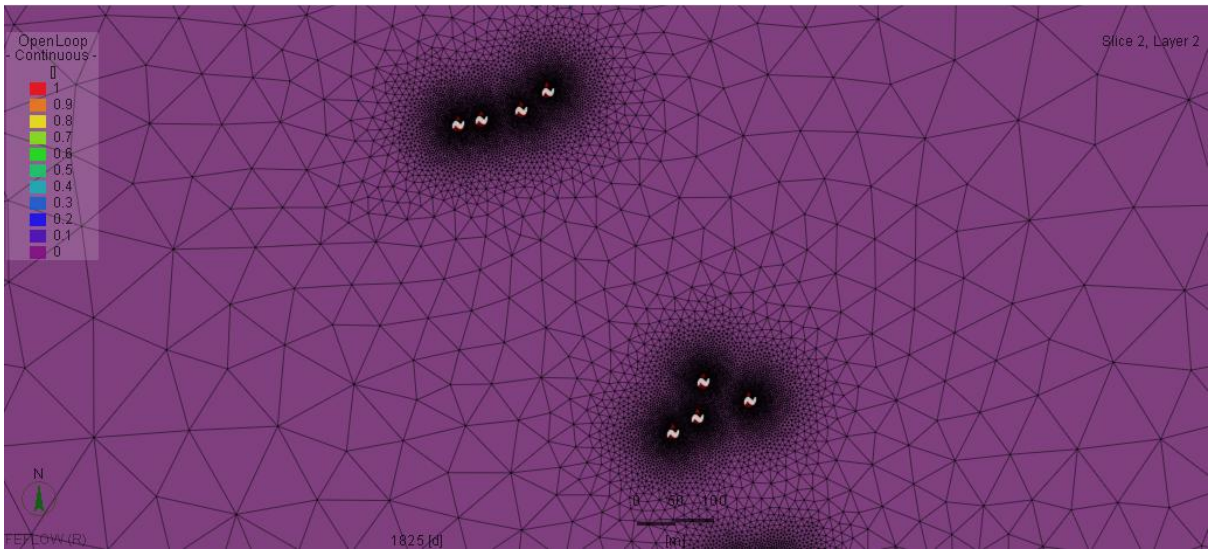

Figure 37 - Open-loop plant system setting.

In FEFLOW, a thermal jump represents the temperature difference across an interface (e.g., at the well–aquifer boundary). In open-loop geothermal systems, when water with a different temperature is injected into the aquifer, the software computes a thermal jump at the injection interface. This approach represents the instantaneous temperature difference between the injected water and the surrounding groundwater, which drives heat transfer into the aquifer. The concept is illustrated in Fig. 32.

3.1.9 Alternative operational scenario

To investigate the impact of well spacing and reinjection density on thermal stability, an alternative operational configuration was implemented. In this scenario, the most densely clustered reinjection wells (Wells 1–4) were deactivated within the Open Loop module, and their associated thermal assignments were removed from the nodal distribution to eliminate residual reinjection effects.

All other hydraulic and thermal boundary conditions, material properties, and time-series inputs were kept unchanged to ensure direct comparability with the base-case scenario. The model was subsequently re-run for the same 20-year simulation period.

The results of this alternative configuration are presented and analysed in Section 3.2.1 to assess its impact on system sustainability.

3.2 Results and analysis

After running the model, the resulting hydraulic head and average temperature histories were obtained.

Fig. 38 shows how the groundwater level (hydraulic head) varies over time at selected points in the model. It illustrates the aquifer's dynamic response to groundwater extraction and reinjection during system operation over the 20-year simulation period.

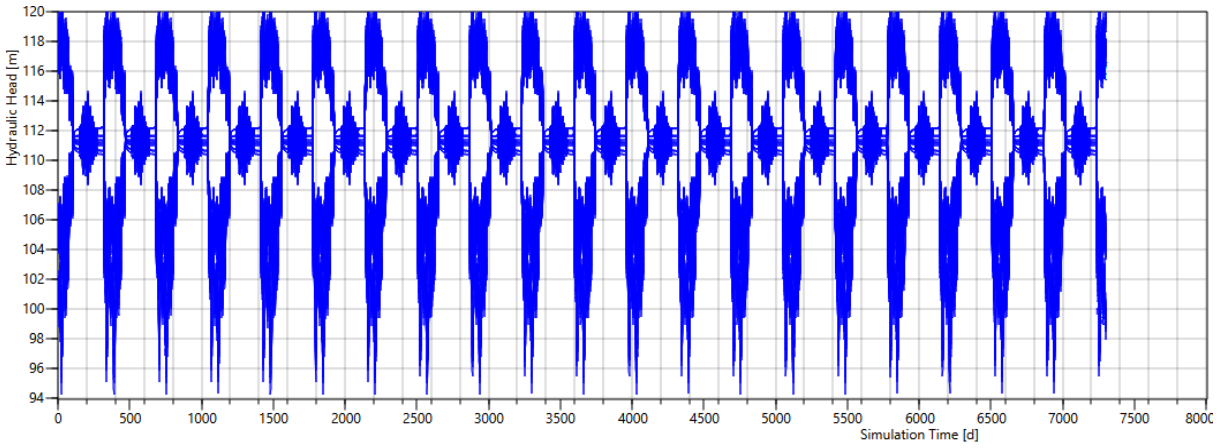

Figure 9 - Groundwater levels at the abstraction and injection wells.

To better illustrate the cyclic hydraulic behaviour and assess the stability of the system, a zoomed view of the final simulation year (Days 6940–7300) is presented in Fig. 39.

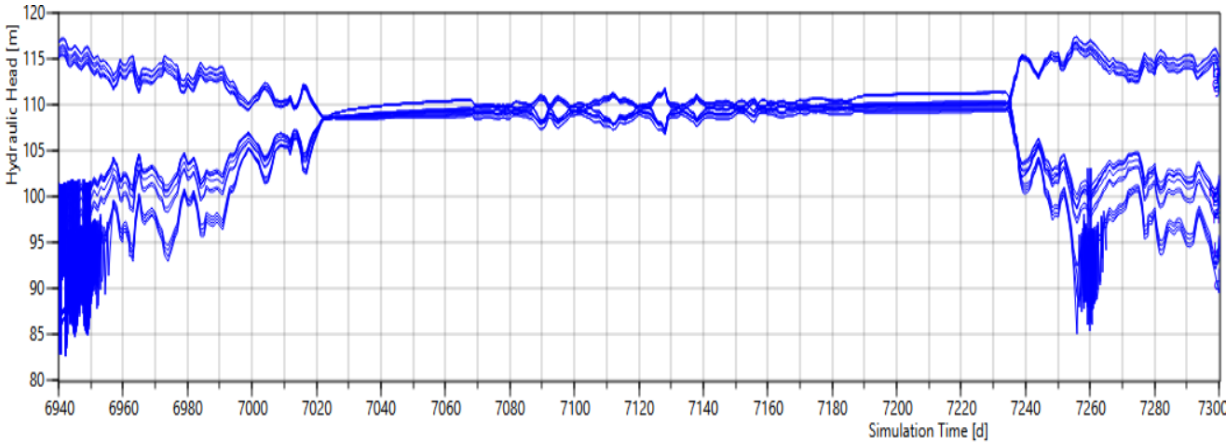

Figure 39 - Zoomed view of hydraulic head variation during the final simulation year.

The head fluctuates periodically between roughly 95 m and 120 m.

The fluctuations match the corresponding pumping/injection operational cycles.

When the pump is running, the water level (hydraulic head) drops, but it quickly returns once pumping stops.

The water level drop (drawdown) stays mostly the same, which indicates the groundwater flow (hydraulic regime) is stable.

The repeated pattern indicates the system has reached a dynamic equilibrium between extraction and reinjection phases.

The moderate and stable hydraulic head variations indicate a well-balanced interaction between pumping and reinjection phases, preventing excessive drawdown or over pressurization of the aquifer.

The consistent head over time confirms the model's correct definition of hydraulic boundaries and aquifer transmissivity. Additionally, the aquifer storage capacity is sufficient to sustain pressure changes without cumulative impacts.

Fig. 40 shows the evolution of the average aquifer temperature over time across the model domain. It illustrates the development of the thermal plume resulting from groundwater extraction and reinjection during system operation.

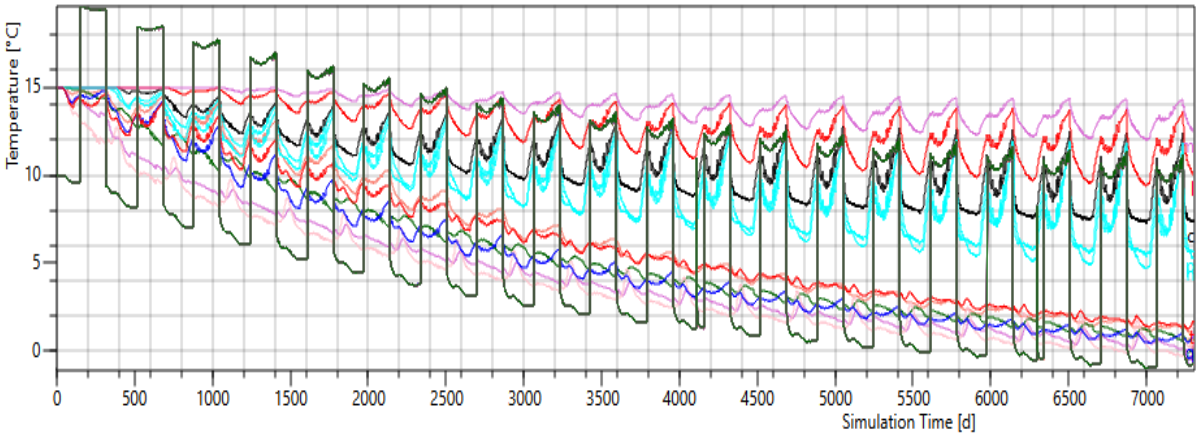

Figure 40 - Groundwater temperature evolution at the abstraction wells (coloured curves) and injection wells (black curves) during the simulation period.

The chart illustrates the periodic cycles of temperature variation over a simulation period of 7,300 days, or 20 years. Throughout this timeframe, all temperature curves exhibit a continuous decline. The initial temperatures start at approximately 15°C, but by the end

of the period, many curves fall to around 1–5°C. Each yearly operating cycle reaches lower minimum temperatures than the previous one, indicating that the system suffers from incomplete recovery and cannot return to its initial temperatures between cycles. Furthermore, the temperature drops during the "on" periods increase over time, while the effectiveness of the "off" periods for recovery diminishes as the aquifer temperature declines. Several curves, particularly the blue and purple ones, show rapid declines, indicating the early arrival of reinjected cold water each year, which leads to thermal interference between the wells.

The operation of the geothermal system is unsustainable for several reasons. First, the long-term periodic reduction in temperature indicates that heat extraction exceeds the thermal recharge capacity of the aquifer, leading to continuous thermal depletion each year since the system does not recycle heat. Additionally, thermal interference between wells is increasing; rapid temperature declines suggest that the reinjected cold water reaches the extraction zones more quickly each year, resulting in short-circuiting and insufficient spacing between wells. Moreover, despite the cycling of the system, the temperature curves do not return to their initial values due to the aquifer's inadequate thermal capacity to handle the imposed load. Consequently, thermal recovery is unlikely, as the draining of thermal energy occurs faster than recharge.

3.2.1 Partial groundwater reinjection option

The alternative operational configuration described in Section 3.1.10 was evaluated to assess its impact on thermal behaviour and long-term system sustainability.

Thermal interference in groundwater systems can arise under various operational conditions. One such condition is very close abstraction-injection pairs, where the short distance allows cold plumes to rapidly reach the abstraction zones. Additionally, dense clusters of wells may cause multiple wells to share the same flow path, leading to significant interference. Furthermore, wells located downgradient from others can receive cooled water from upstream wells, resulting in thermal drift. Lastly, high pumping or reinjection rates can exacerbate thermal loading within the aquifer, further contributing to thermal interference.

Based the map of (Figure -Abstraction and injection wells within the studies city.), the most densely clustered reinjection wells (Red Wells 1–4) were deactivated, as their

spatial arrangement and local flow direction could potentially drive the cooled thermal plume toward neighbouring abstraction wells.

The nodal distribution within the Open Loop module was subsequently updated to eliminate residual reinjection effects. In this modified configuration, a portion of the abstracted water was assumed to be discharged to surface channels rather than reinjected into the aquifer.

The simulation was then re-run under the same hydraulic and thermal boundary conditions for the same 20-year period. The resulting temperature response is shown in Fig. 41.

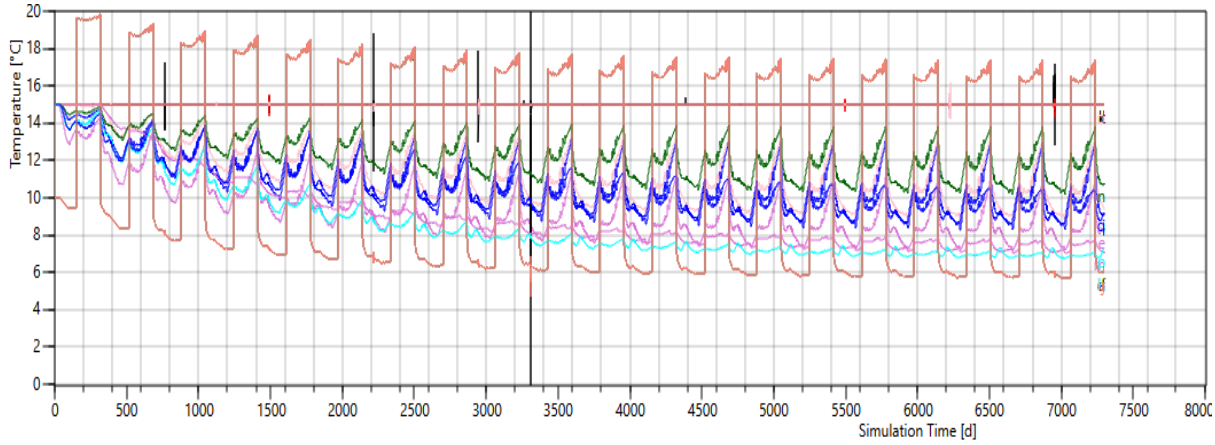

Figure 41 - Average temperature of aquifer after disactivating reinjection wells 1-4.

To further assess the seasonal thermal response, a zoomed view of the final simulation year is shown in Fig. 42.

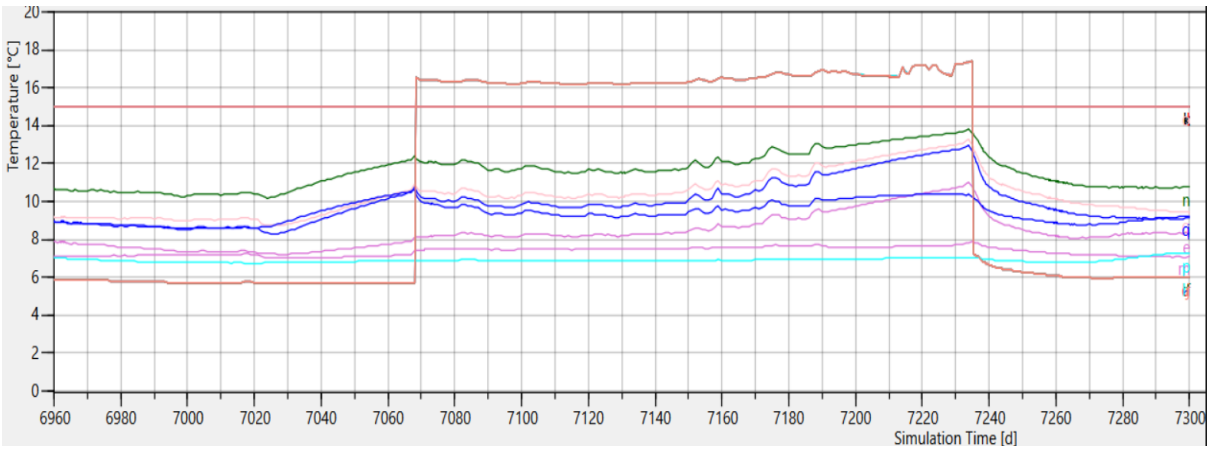

Figure 42 - Zoomed view of the average aquifer temperature during the final simulation year.

The updated configuration demonstrates a clear improvement in system behaviour. The temperature curves exhibit stable periodic seasonal fluctuations that remain consistent throughout the simulation period.

No cumulative cooling trend is observed, and temperatures recover annually to approximately the same levels (no thermal drift).

Minor transient numerical anomalies occur at operational switching points due to abrupt boundary condition changes imposed at discrete time steps and the linear interpolation of time-series inputs. Such short-lived oscillations are inherent to transient numerical simulations and do not affect the long-term thermal behaviour or stability of the aquifer system.

The cyclic patterns (box-shaped red lines) represent seasonal operational phases: higher temperatures during summer injection (approximately 14–16 °C) and lower temperatures during winter injection (approximately 8–11 °C). These values are consistent with realistic seasonal groundwater temperature variations in Milan.

This contrasts sharply with the initial scenario (Figure), which showed a continuous temperature decline (temperatures dropped to 0–2 °C) due to strong thermal interference. The absence of long-term drift confirms that the modified configuration mitigates thermal interference and supports sustainable long-term open-loop geothermal operation.

4 Conclusions

The numerical flow and heat transport simulation of a shallow geothermal district heating and cooling system for the Città Studi area in Milan comes with valuable insights into the long-term thermal and hydraulic behaviour of the local shallow geothermal system. The aim was to assess if the aquifer can support the required extraction-injection thermal loads over a 20-year operational period in a sustainable way.

The hydraulic outcomes show a stable and sustainable response of the aquifer under the operating conditions. Hydraulic heads exhibit periodic fluctuations which are fully consistent with the pumping and injection schedule and there isn't a sign for long-term downward or upward trends. The absence of cumulative drawdown indicates that the aquifer possesses sufficient transmissivity and storage capacity to meet the hydraulic stresses without risk of depletion or over-pressurization.

In contrast, the thermal outcomes show obviously pattern of progressive thermal depletion. Monitored temperatures show a continuous decline during the simulation, with values decreasing from initial conditions of 15 °C to as low as 0–2 °C by the end of the simulation period.

To address this issue, a model optimisation process was performed. Reinjection wells 1–4, located in the highest interference zone, were removed from the system. Part of the discharged water was diverted to surface channels so that it does not re-enter the aquifer. Consequently, the corresponding thermal and hydraulic assignments were also removed from the Open Loop nodal distribution.

The new configuration was then re-run. The updated results showed a clear improvement: groundwater temperatures exhibited consistent seasonal oscillations without any long-term cooling trend, unlike the initial scenario. A thermal equilibrium was achieved, with annual heat recovery remaining balanced and temperatures staying stable throughout the entire simulation period. The hydraulic response was already stable initially and remained unchanged after the optimization.

Thus, the optimized well configuration of the model ensures a stable and sustainable long-term geothermal performance.

References

1. European Commission, Joint Research Centre, Institute for Environment and Sustainability, & European Technology Platform on Renewable Heating and Cooling. (2011). *2020–2030–2050: Common vision for the renewable heating and cooling sector in Europe*. Luxembourg: Publications Office of the European Union.

2. International Renewable Energy Agency (IRENA). (2023). *Global geothermal market and technology assessment* and Eurostat (Energy statistical country datasheets).

3. European Technology Platform on Renewable Heating and Cooling. (2011). *2020–2030–2050: Common vision for the renewable heating and cooling sector in Europe*.

4. Carapezza, M. L., et al. (Year). *Assessment of a low-enthalpy geothermal resource and evaluation of the natural CO_2 output in the Tor di Quinto area (Rome city, Italy)*.

5. National Institute of Advanced Industrial Science and Technology (AIST). (n.d.). *(FREA)*. Retrieved from https://www.aist.go.jp/fukushima/en/.

6. Casasso, A. RER03_Heat Pumps. *Renewable Energy Resources, Politecnico di Torino*.

7. Module 4: Heat pump technology - CIBSE Journal.

8. Automatic Heating Global Pty Ltd (2025). *"Heat Pump Efficiency"*.

9. Muhunthan, B., & Wen, S. (Year). *Analysis of geothermal pile foundations under axial loading (2013)*.

10. D2 Parametre ved Design af Jordvarmeanlaeg (ver 0). (n.d.). *Technical guidelines for ground source heat pump design*.

11. ESG Economist. (Year). *Geothermal energy has great potential but there are challenges*.

12. International Geothermal Association. (2000). *Standard geothermal data report*. Available at: https://www.lovegeothermal.org/pdf/IGAstandard/WGC/2000/R0090.PDF.

13. Garzanti, E., et al. (2011); Scardia, G., et al. (2012).

14. Regione Lombardia & ENI (2002); Martinis & Mazzarella (1971). *Acquifero Profondo*.

15. Zhu, K., et al. (Year). *Characterization of the subsurface urban heat island and its sources in the Milan city area, Italy*.

16. Colombo, L., et al. *The groundwater rise in the urban area of Milan (Italy) and its interactions with underground structures and infrastructures. Engineering Geology,* Elsevier.

17. Università degli Studi di Milano-Bicocca. *Analysis of groundwater environment change in the Milan Metropolitan area by hydro stratigraphic, groundwater quality and flow modelling.*

18. De Caro, M., Crosta, G. B., & Previati, A. *Modelling the interference of underground structures with groundwater flow and remedial solutions in Milan*. Available at: https://www.elsevier.com/locate/enggeo.

19. Vagnon, F. *Geothermal energy: Ground source heat pump systems and open loop systems. Politecnico di Torino.*

20. Casasso, A. *Introduction to geothermal energy and Open loop shallow geothermal systems* In *Renewable Energy Resources, Politecnico di Torino.*

21. DHI-WASY GmbH. (2019). *FEFLOW 7.2 User Manual: Time Series*. Berlin, Germany.

22. Politecnico di Milano. (2020, August 6). *Le azioni proposte dal Politecnico di Milano per il governo della mobilità.* Campus Sostenibile – Servizio Sostenibilità. Available at: https://www.campus-sostenibile.polimi.it/wp-content/uploads/2023/08/allegato1_le-azioni-proposte-dal-Politecnico.pdf.

23. ICLEI – Local Governments for Sustainability. (2019). *Milan: Case study – Energy, decarbonization, urban regeneration (Urban-LEDS).* Available at: https://urban-leds.org/wp-content/uploads/2019/resources/case_studies/ICLEI_cs_milan-case-study.pdf.